AD-A048 895 AIR FORCE INST OF TECH WRIGHT-PATTERSON AFB OHIO SCH--ETC F/G 20/4
ANALYSIS AND DESIGN OF A COOLED SUPERCRITICAL AIRFOIL TEST MODE--ETC(U)
DEC 77 R G POPE

UNCLASSIFIED AFIT/GAE/AA/77D-11 NL

1 of 2
ADA048 895

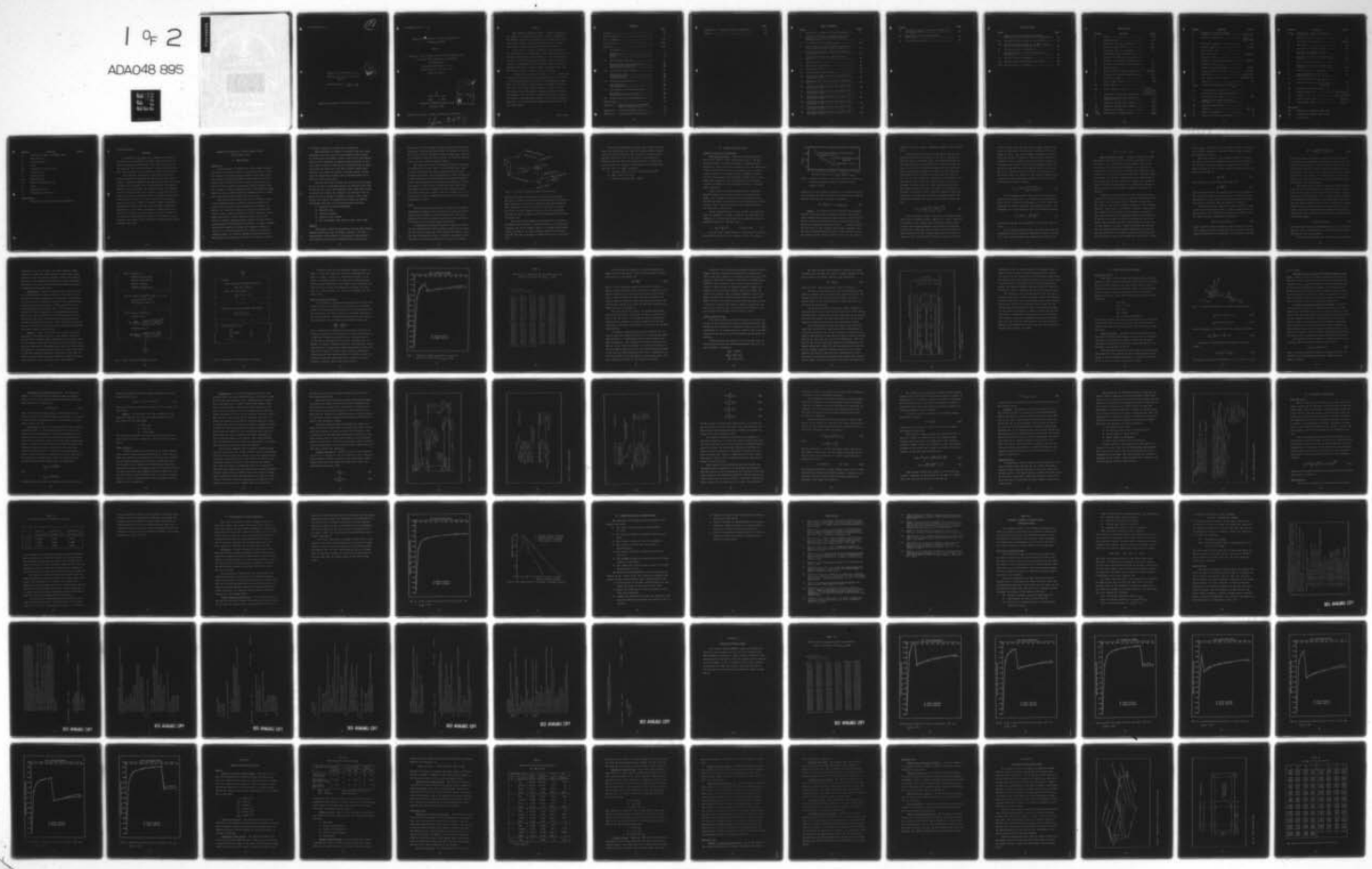

AFIT/GAE/AA/77D-11

ANALYSIS AND DESIGN OF A COOLED SUPERCRITICAL AIRFOIL TEST MODEL

THESIS

AFIT/GAE/AA/77D-11 Ray G. Pope
Capt USAF

AFIT/GAE/AA/77D-11

ANALYSIS AND DESIGN OF A COOLED SUPERCRITICAL AIRFOIL TEST MODEL

THESIS

Presented to the Faculty of the School of Engineering
of the Air Force Institute of Technology
Air University
in Partial Fulfillment of the
Requirements for the Degree of
Master of Science

by
Ray G. Pope, B.S.
Capt USAF
Graduate Aeronautical Engineering
December 1977

(See 1473)

Preface

The purpose of this study was to design a supercritical airfoil test model which would be used to investigate the effects of cooling on boundary layer stability in subsonic flow. Previous investigations have indicated that transition to turbulent flow was delayed by cooling.

This report is limited in scope to the model design and test parameter specification. I hope that this work will be found complete and self-sufficient by the student who undertakes the actual testing of the model. Anyone who is interested in determining the heat transfer for flow over an arbitrary body with constant surface temperature will find the computer program in Appendix A to be useful.

I would like to thank my advisors, Dr. J. E. Hitchcock of the Air Force Institute of Technology and Dr. A. W. Fiore of the Flight Dynamics Laboratory at Wright-Patterson AFB, Ohio, who have given timely guidance essential to the completion of this study. Deep gratitude is also expressed to F.W. Spaid, Senior Scientist at McDonnell Douglas Research Laboratories, for his effort in providing me with experimental pressure distributions. Lastly, I wish to acknowledge my gratitude to my wife for her inspiration and effort in typing this thesis.

Ray G. Pope

Contents

List of Figures

List of Tables

Nomenclature

Symbols	Quantity	Units
A	Area	$in.^2$
a	Elemental area	$in.^2$
a	Semi-major axis of an ellipse	in.
a	Speed of sound, $\sqrt{\gamma RT}$	ft/sec
b	Semi-minor axis of an ellipse	in.
C	Aerodynamic force coefficient	
C_p	Pressure coefficient, $(p-p_\infty)/q$	
C_x	Location of centroid in x-direction	in.
C_y	Location of centroid in y-direction	in.
c	Airfoil chord	ft
c_p	Specific heat at constant pressure	$B/(lb_m-R)$
$\tilde{c}$	Location of fiber from neutral axis	in.
D	Drag force, $C_d qS$	lb_f
F	Force, normal force	lb_f
FS	Safety factor	
g_o	Newton constant (32.174)	$\frac{ft\text{-}lb_m}{(lb_f\text{-}sec^2)}$
h	Convective conductance coefficient	$B/(sec\text{-}ft^2\text{-}R)$
I	Moment of inertia with respect to neutral axis	$in.^4$
I_x	Moment of inertia about x-axis	$in.^4$
I_y	Moment of inertia about y-axis	$in.^4$
I_{xy}	Product of inertia	$in.^4$
Δi_{fg}	Latent heat of vaporization	B/lb_m

Symbols	Quantity	Units
J	Mechanical to thermal energy conversion factor (778.16).....	$(ft\text{-}lb_f)/B$
k	Thermal conductivity.....	$\frac{B\text{-}ft}{(sec\text{-}ft^2\text{-}R)}$
L	Lift force, $C_l qS$.....	lb_f
M	Moment, $C_m qSc$.....	$ft\text{-}lb_f$
M	Mach number, u/a.....	
$\dot{m}$	Mass flow rate.....	lb_m/sec
N	Summation limit.....	
P	Pressure, force per unit area.....	lb_f/ft^2
Pr	Prandtl number, $\mu c_p/k$.....	
Q	Total heat transfer rate.....	B/sec
q	Dynamic pressure, $\rho u_\infty^2/2$.....	lb_f/ft^2
$\dot{q}''$	Heat flux.....	$B/(sec\text{-}ft^2)$
R	Gas constant for air (1716).....	$ft^2/(sec^2\text{-}R)$
R	Radius.....	ft
R_{crit}	Critical Reynolds number, $\sqrt{Re_{x_{crit}}}$.....	
Re	Reynolds number, $\rho ux/\mu$	
r	Recovery factor, $(T_{aw}-T_e)/(T_o-T_e)$.....	
S	Airfoil planform area.....	ft^2
SR	Safety ratio, stress to material strength.....	
St	Stanton number, $h/\rho u c_p$	
T	Torque.....	$in.\text{-}lb_f$
T	Static temperature.....	R
T^*	Eckert's reference temperature.....	R

Symbols	Quantity	Units
T_w/T_∞	Cooling ratio, wall to freestream temperature.....	
t	Thickness normal to chord.....	in.
u	Velocity in x-direction.....	ft/sec
V	Shear force.....	lb_f
X	Distance along airfoil chord.....	in.
x	Distance from stagnation point parallel to surface.....	ft
x	Distance to center of element along x-axis.....	in.
Y	Distance normal to chord.....	in.
y	Distance to center of element along y-axis.....	in.
z	Axis perpendicular to x-axis.....	in.
α	Angle of attack of chord w.r.t. undisturbed flow.....	o
γ	Ratio of specific heats, c_p/c_v.....	
Δ_2	Enthalpy thickness, $\frac{\int_o^\infty u(T - T_\infty)dy}{u_\infty(T_w - T_\infty)}$ ...	ft
Δ_4	Conduction thickness, k/h_x.....	ft
μ	Dynamic viscosity.....	$(lb_f\text{-sec})/ft^2$
ρ	Density.....	$(lb_f\text{-sec}^2)/ft^4$
σ	Normal stress, F/A.....	$lb_f/in.^2$
τ	Shear stress, V/A.....	$lb_f/in.^2$

Subscripts

aw	Evaluated at adiabatic wall state
c/4	Evaluated at quarter chord point
d	Section drag

Symbols	Quantity	Units
e	Evaluated at edge of boundary layer	
f	Skin friction	
i	Summation index	
L	Lower	
LE	Evaluated at leading edge	
l	Section lift	
m	Section moment	
max	Maximum value	
o	Total or stagnation value	
U	Upper	
w	Evaluated at wall	
∞	Evaluated at freestream	

Superscripts

*	Evaluated at Eckert's reference temperature

Abstract

A wind tunnel test model of a supercritical airfoil was designed to investigate the wall cooling effect on subsonic boundary layer stability. A DSMA 523 airfoil section was employed. The model was designed to have surface temperature instrumentation and a liquid nitrogen cooling system.

Heat transfer, aerodynamic loads and stresses, and instrumentation were analyzed for the proposed test conditions. A computer program was developed to analyze the forced, convective heat transfer over a two-dimensional body with a constant wall temperature. The program utilized an integral method to compute local Stanton numbers. Local heat flux and total heat flow were predicted for a Mach number of 0.7, Reynolds numbers of 0.923×10^6 and 1.673×10^6, and cooling ratios from 1.000 to 0.824. The stress analysis consisted of applying beam bending theory, along with some simplifying assumptions, to the model. Construction drawings and specified test conditions for Mach numbers of 0.3, 0.5, and 0.7 are included. The proposed tests are to be conducted in the subsonic test section of the Trisonic Test Facility at Wright-Patterson AFB, Ohio.

Analysis and Design of a Cooled Supercritical Airfoil Test Model

I. Introduction

Background

In 1974 Boehman and Mariscalco of the Dayton Research Institute, University of Dayton, Dayton, Ohio began to study the problem of determining the conditions under which flow in a cooled compressible laminar boundary layer becomes unstable (Ref 2). This research was under contract from the Air Force Flight Dynamics Laboratory, Wright-Patterson AFB, Ohio. Using a computer program developed from parallel linear stability theory, Boehman looked at boundary layers in shock tube induced flow and subsonic wind tunnel flow.

This theoretical problem is still not totally solved. A full description of the stability problem requires the solution of the Navier-Stokes equations with boundary conditions for transition. This set of equations has not been solved to date. Even linearization of these equations using small perturbation theory yields equations that are not solvable. Finally, Boehman further assumed that the flow is locally parallel and reduced the problem to a single ordinary differential equation. He found that moderate cooling resulted in a significant increase in stability of subsonic boundary layers. As a result, Boehman recommended that an experimental test program be developed to study the effects

of surface cooling on boundary layer transition.

Experimentation is needed to correlate with the linear stability theory and validate the assumptions made during the development of Boehman's theory. Very little experimental work has been performed on boundary layer stability in subsonic flows. However, there has been extensive work in supersonic flow and shock tube flow (Ref 16 and 3) which gives insight to the stability problem. Although similar results would be expected for subsonic flow, experimentation is required to confirm this fact.

The fact that skin friction and the rate of heat transfer are an order of magnitude greater in turbulent flow than in laminar flow at the same Reynolds number makes the ability to predict and control the transition to turbulent flow of great use in the design of aerospace vehicles. Most importantly, the control of transition will result in reduced aerodynamic drag with the following possible benefits:

1. Increased aircraft performance
2. Extended range
3. Increased payload
4. Improved fuel economy
5. Use of hydrogen fuel feasible (fuel cools wing)

Problem

The problem, which was proposed by the Air Force Flight Dynamics Laboratory, was to design, construct, and test a supercritical airfoil model in the subsonic test section of the Trisonic Test Facility at Wright-Patterson AFB, Ohio.

The test was to investigate the wall cooling effect on boundary layer stability and transition. The purpose of the test was to increase the understanding-of boundary layer stability, to obtain clues that might advance the stability theory, and to correlate with the present theory.

The model was to have a DSMA 523 airfoil section with the capability of being cooled. This Whitcomb-type, supercritical airfoil profile was developed by the McDonnell Douglas Corporation. The non-dimensional surface coordinates of this airfoil were obtained from Ref 8:738. The angle of attack was eliminated as a variable by specifying a constant zero angle for the airfoil section chord line. This model was required to have a constant airfoil section, to span the entire 24 in. wind tunnel, and to be mounted on two "L" shaped struts. Major components of the model and struts are illustrated in Fig 1.

Scope

The problem was divided into two phases. The present investigation completed the analysis and design phase which included specification of testing procedures. The second phase which consists of model construction and testing will be performed as a separate independent study.

An analytical study was required to design the model and its cooling system. This analysis required the solution for the forced, convective heat transfer in subsonic flow over the two-dimensional wing. A computer program was developed from the reference temperature approach to variable

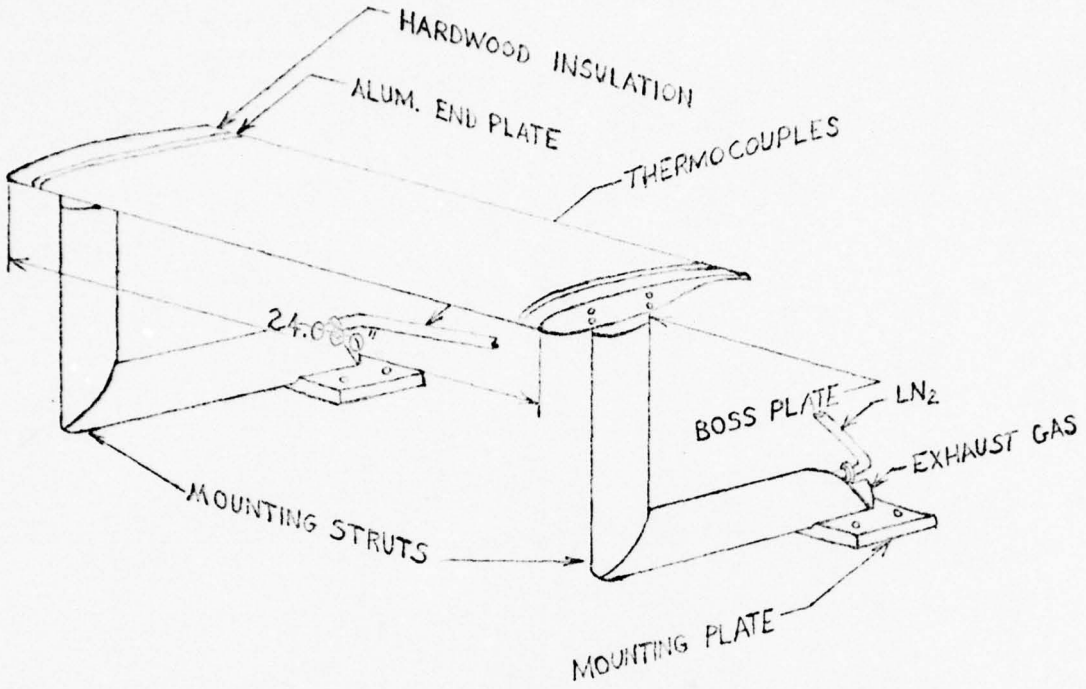

Fig. 1 Concept of the Model with Mounting Struts

property flow which used integral equations to determine the local, laminar and turbulent Stanton numbers for constant wall temperature flow over an arbitrary body (Ref 9:226 and 247). Estimates of heat conduction in the model were also necessary. The heat transfer analysis which was performed for only the most stringent test conditions appears in detail in Section II.

The model design required determination of the forces and moments on the model, a stress analysis, and construction drawings. The stress analysis made use of simple beam bending theory. Details of the stress analysis which was performed only for the most stringent test conditions appear in Section III.

The test was designed to measure the movement of boundary layer transition as a function of wall cooling relative to the no cooling condition. The stability results of Boehman (Ref 2:57) were used in the forced, convective heat transfer analysis. The test conditions which are specified in Section IV were limited to combinations of the following variables for the ranges indicated:

1. Reynolds number (1.673×10^6 and 0.923×10^6)
2. Mach number (0.7-0.3)
3. Cooling ratios (1.000 - 0.824)

II. Heat Transfer Analysis

Boundary Layer Forced Convection

General Assumptions. Simplifying assumptions were made to the model so that existing solutions to the heat transfer problem could be used. With the proposed model description, the fluid flow was assumed to be two-dimensional. It was assumed that only the most stringent test condition of M=0.7 needed to be analyzed since aerodynamic heating and heat flux increase as a function of Mach number. A constant wall temperature was specified since it eliminated temperature gradients as an influencing factor in boundary layer transition.

Boehman reported results that give the transition Reynolds number as a function of the wall cooling ratio, T_w/T_∞ , for a family of subsonic Mach numbers (Ref 2:57). The results apply to a flat plate. It was assumed that these results (Fig 1) could be used as a first approximation to the transition on the model.

At the stagnation point on the airfoil, the equations used were singular. In order to compute the convective conductance, h, the flow was assumed to be approximated by the potential flow over a cylinder (Eq 1).

$$u_e = 2\, u_\infty\, x/R \qquad (x/R << 1.0) \qquad (1)$$

For the range of Mach numbers of interest, M=0.3 to 0.7, compressibility could not be neglected. Thus, the flow was

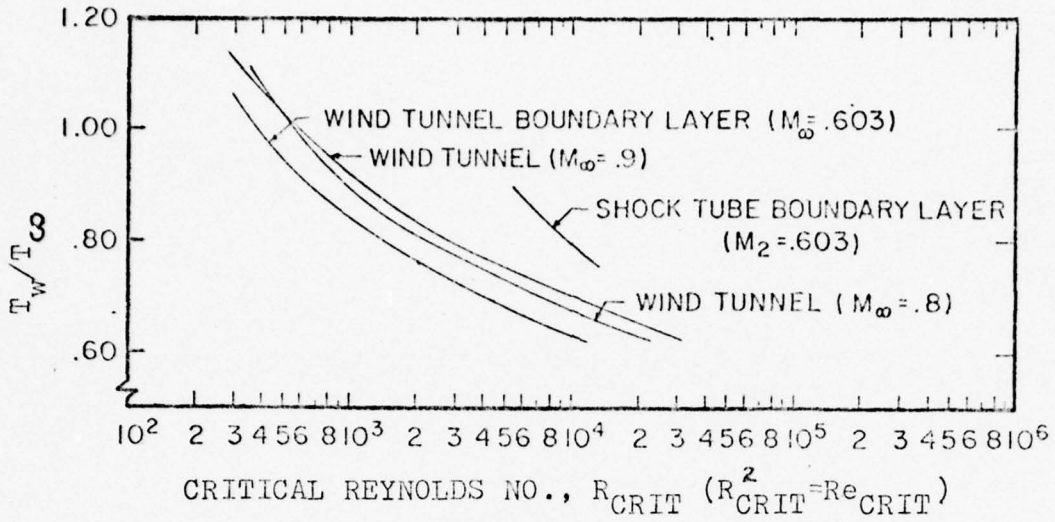

Fig. 2 Relative Stability of Boundary Layers as a Function of Critical Reynolds Number and Cooling Ratio (From Ref 2:57)

considered to have variable properties. A reference temperature approach was used in which all properties were computed locally using Eckert's reference temperature,

$$T^* = \frac{T_w + T_e}{2} + 0.22(T_{aw} - T_e) \qquad (2)$$

Theory. The solution to the convective heat transfer analysis could have been obtained by solving the boundary layer momentum equation which establishes the velocity field and then solving the boundary layer energy equation. This method was complicated, and the accuracy of results required did not merit its use. Simpler methods were available when the proper approximations were made to the problem. Use of the simpler methods required that the flow over the model be

analyzed in three regions, stagnation, laminar, and turbulent flow.

Kays (Ref 9:223) developed a method of computing the local Stanton number for laminar flow over a constant temperature body of arbitrary shape. This method was based on the assumption that the variation of conduction thickness, Δ_4, for flow over an arbitrary shape was of the same form as the similarity solutions for wedge flow. The function, which expressed the variation of conduction thickness in air, Pr= 0.7, for wedge flow, was defined numerically. Smith and Spalding (Ref 13:60) approximated this function by a straight line which fits the wedge solutions exactly for the stagnation point and the flat plate. The resulting expression was solved for the conduction thickness. Using the definition of conduction thickness and Stanton number, the following expression was derived for the local Stanton number:

$$St_{x_{Lam}} = \frac{0.418 \, {}^{*}\mu^{0.5} \, ({}^{*}\rho u_e)^{0.435}}{\left[\int_0^x ({}^{*}\rho u_e)^{1.87} dx \right]^{0.5}} \qquad (3)$$

For the turbulent case of flow over a constant temperature body of arbitrary shape, Ambrok (Ref 1:1979) suggested a solution of the integral energy equation without having to solve the momentum equation. This method was developed by Kays (Ref 9:245-247). Kays started with the solution to heat convection for the constant temperature flat plate in turbulent flow. This solution which was expressed in terms

of the Stanton number was used in the energy integral equation for a flat plate to develop an expression for the enthalpy thickness, Δ_2. The resulting relationship between x and Δ_2 was used to develop a Stanton number which was a function of local parameters only. This Stanton number relationship was assumed to hold for any turbulent flow. The general energy equation was integrated with the heat flux, $\dot{q}''_w$, in the equation expressed in terms of the convective conductance which was found from the assumed Stanton number relationship. The resulting expression was solved for the following local Stanton number:

$$St_{x_{Tur}} = 0.0295 \frac{Pr^{-0.4} \mu^{*0.2}}{\left[\int_0^x \rho^* u_e \, dx\right]^{0.2}} \qquad (4)$$

At the stagnation point, Eq 3 for the local Stanton number did not apply since $u_e=0$. However, Eq 3 was used to solve for the convective conductance, h, at x=0. After substituting the assumed velocity relationship from Eq 1, the expression for h was integrated with the following results:

$$h_x = 1.001 \, c_p \sqrt{\frac{u_\infty \rho^* \mu^*}{R}} \qquad (5)$$

The value of h_x was now independent of the values, x=0 and $u_e=0$.

In all three regions of flow, the local heat flux was determined from the convective conductance obtained from Eq 3, 4, and 5 and the known local temperature difference by

$$\dot{q}''_w = h_x (T_w - T_{aw}) \qquad (6)$$

Computer Program Logic. A computer program call CONHEAT was written to analyze the forced, convective heat transfer on the airfoil model. This program utilized Eq 2 through Eq 6. The program was designed to be general in nature and could be utilized to compute the convective heat transfer for any two-dimensional body with a constant surface temperature. Any further restrictions on the application of the program will be noted during the discussion of program logic. A detailed description of the input/output format is given in Appendix A along with a complete listing of the program.

Information required to solve the convection problem included freestream conditions, a pressure distribution over the model, model geometry, and the desired cooling ratio. The required freestream conditions consisted of the velocity, pressure, temperature, and viscosity. Pressure coefficients were required on the surface at intervals of 5 percent of the chord starting at the stagnation point. This resulted in 21 points on the upper surface and 21 points on the lower surface being defined for use in determining the total rate of heat transfer. A surface coordinate system was defined, and the distance between pressure coefficients on the surface was determined. Additional geometry required included the chord length, span, and leading edge radius. The cooling

ratio, T_w/T_∞ , specified the surface temperature for the given freestream temperature, and the critical Reynolds number was obtained from Fig 2.

The first section of the program computed the properties at the discrete locations of the pressure coefficients for the upper and lower surfaces in addition to the freestream density and the recovery factors. The laminar recovery factor was defined by

$$r_{Lam} = \sqrt{Pr} \tag{7}$$

The turbulent recovery factor was defined by

$$r_{Tur} = \sqrt[3]{Pr} \tag{8}$$

The freestream density was computed from the perfect gas law. The velocity, temperature, and pressure at each point were determined by using inviscid relations which did not include the effect of boundary layer displacement thickness.

The second section computed the Eckert reference temperature and the properties based on this temperature for the upper surface. The adiabatic wall temperature which is used to compute Eckert's temperature was found by

$$T_{aw} = T_e + r u_e^2 / 2 c_p g_o J \tag{9}$$

where r was the value for laminar flow from Eq 7. Then Eckert's temperature was computed from Eq 2. The viscosity was computed using Eckert's temperature in Sutherland's equation,

$$\mu^* = \mu_\infty \left(\frac{T^*}{T_\infty}\right)^{3/2} \left(\frac{T_\infty + 198.72}{T^* + 198.72}\right) \qquad (10)$$

The local density was computed using the perfect gas law. A local Reynolds number was computed and compared with the critical Reynolds number. If the value of the critical Reynolds number had been exceeded, then the computations were repeated with the value of r defined by Eq 8 for the remaining points on the surface in turbulent flow. For the third section, the same procedures as in the second section were repeated for the lower surface.

The fourth section computed the local Stanton number, local convective conductance, and local heat flux at each point on the upper surface, Equation 5 was used to compute the convective conductance at the stagnation point. Equation 3 was numerically integrated by the trapezoidal rule to obtain the laminar Stanton number. After the critical Reynolds number had been exceeded, Eq 4 was used instead of Eq 3 to compute the local turbulent Stanton number. The following relation was used to compute the convective conductance from the Stanton number:

$$h_x = St_x \, \rho^* \, u_e \, c_p \qquad (11)$$

The local heat flux was determined from Eq 6. For the fifth section, the same procedures as in the fourth section were repeated for the lower surface.

The last section integrated the local heat flux by the

trapezoidal rule for the upper and lower surfaces. These results were added for both surfaces with the final result being the total rate of heat transfer. Other results which were part of the program output were the local conditions at each point and a plot of the heat flux distribution. Figure 3 summarizes the program logic.

Design Data. The most stringent test condition determined the design data which was used. A Mach number of 0.7 was selected. This corresponded to a velocity of 813 ft/sec at the wind tunnel temperature of 100 F. The freestream viscosity from Eq 10 was 0.37049×10^{-6} lb_f-sec/ft^2. The freestream pressure was determined from a method described in Section IV. This pressure and the corresponding Reynolds number were 1320 lb_f/ft^2 and 1.673×10^6 respectively. The desired cooling ratio was 0.620. The airfoil geometry was obtained graphically from a full scale drawing of the airfoil section. The last item required was the pressure distribution which was obtained from Ref 8:739.

Results. A plot of the heat flux for Re=1.673×10^6 and T_w/T_∞ =0.620 appears in Fig 4. The negative values of the heat flux indicated heat transfer from the boundary layer to the airfoil. There was a large flux near the leading edge which was expected for the stagnation region. The flux dropped off quickly in the laminar flow region. The jump in heat flux at x/c=0.25 indicated transition to turbulent flow. The turbulent heat flux which was larger than the laminar flux gradually decreased to the trailing edge of the airfoil.

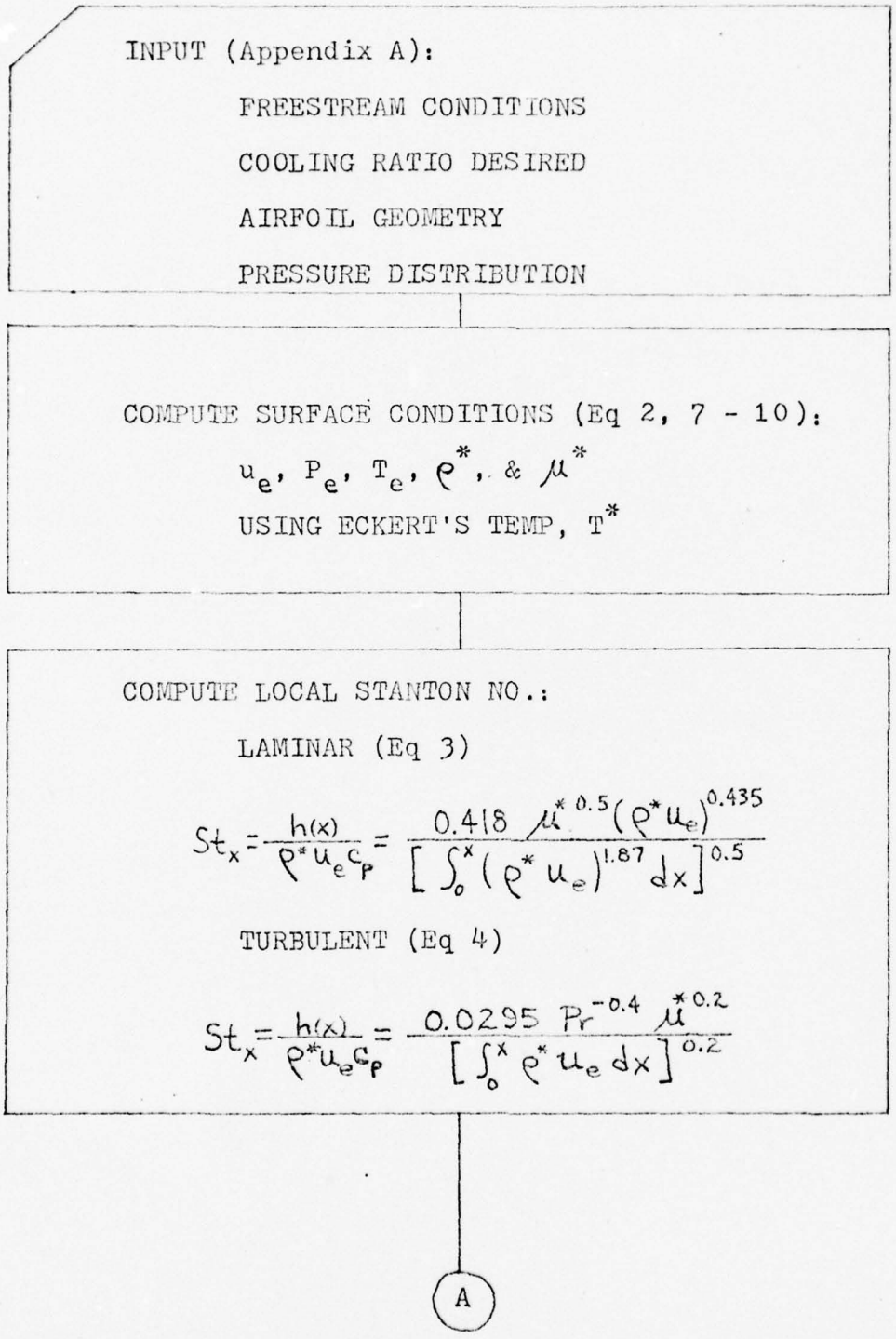

Fig. 3 Flow Diagram for CONHEAT Program

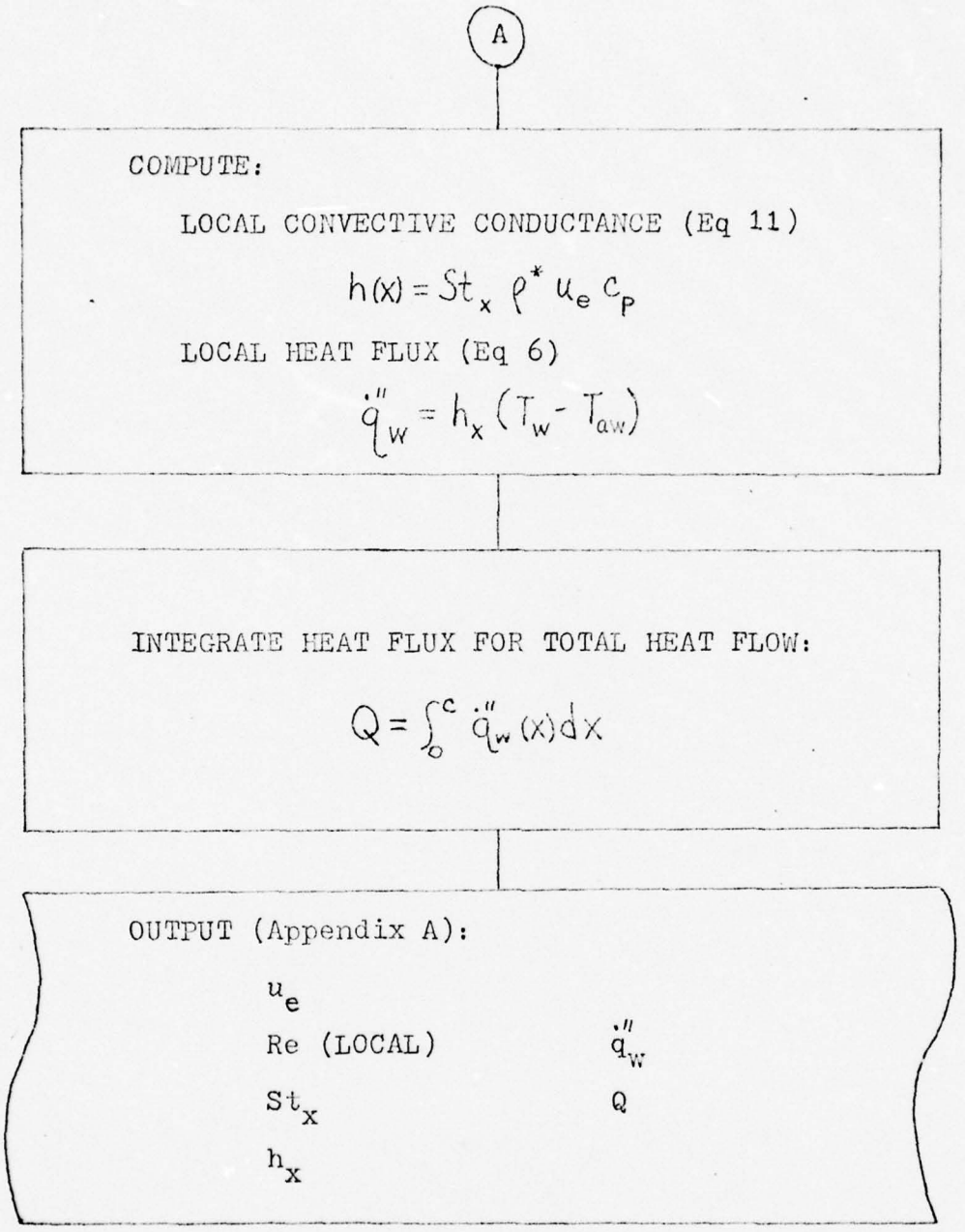

Fig. 3 (continued) Flow Diagram for CONHEAT

Further results of the convection analysis appear in Table I. This table describes the local conditions for the upper and lower surfaces as a function of location in the surface coordinate system. The convective conductance and Stanton number followed the same trend as was noted for the heat flux. As a result of integrating the local heat flux over the airfoil surface, the total heat transfer rate was 17.03 B/sec.

Heat Conduction Estimates

Heat conduction estimates were performed to aid in the proper selection of construction materials for the airfoil surface and insulating end sections and to determine the proper thicknesses for these materials. A detailed analysis of the steady state heat conduction problem would have required the solution of the two-dimensional Laplace's equation,

$$\frac{\partial^2 T}{\partial x^2} + \frac{\partial^2 T}{\partial y^2} = 0$$

for a constant wall temperature and specified heat flux as boundary conditions. The distribution of heat flux varies as a function of freestream conditions and cooling ratio as can be seen in Appendix B. Thus, after a solution was obtained, it would be valid for only one test condition. Using this solution to design the constant temperature airfoil surface would result in a model with a constant temperature surface only at that test condition. In addition, model construction would be complicated by the contoured surfaces required to achieve the constant temperature.

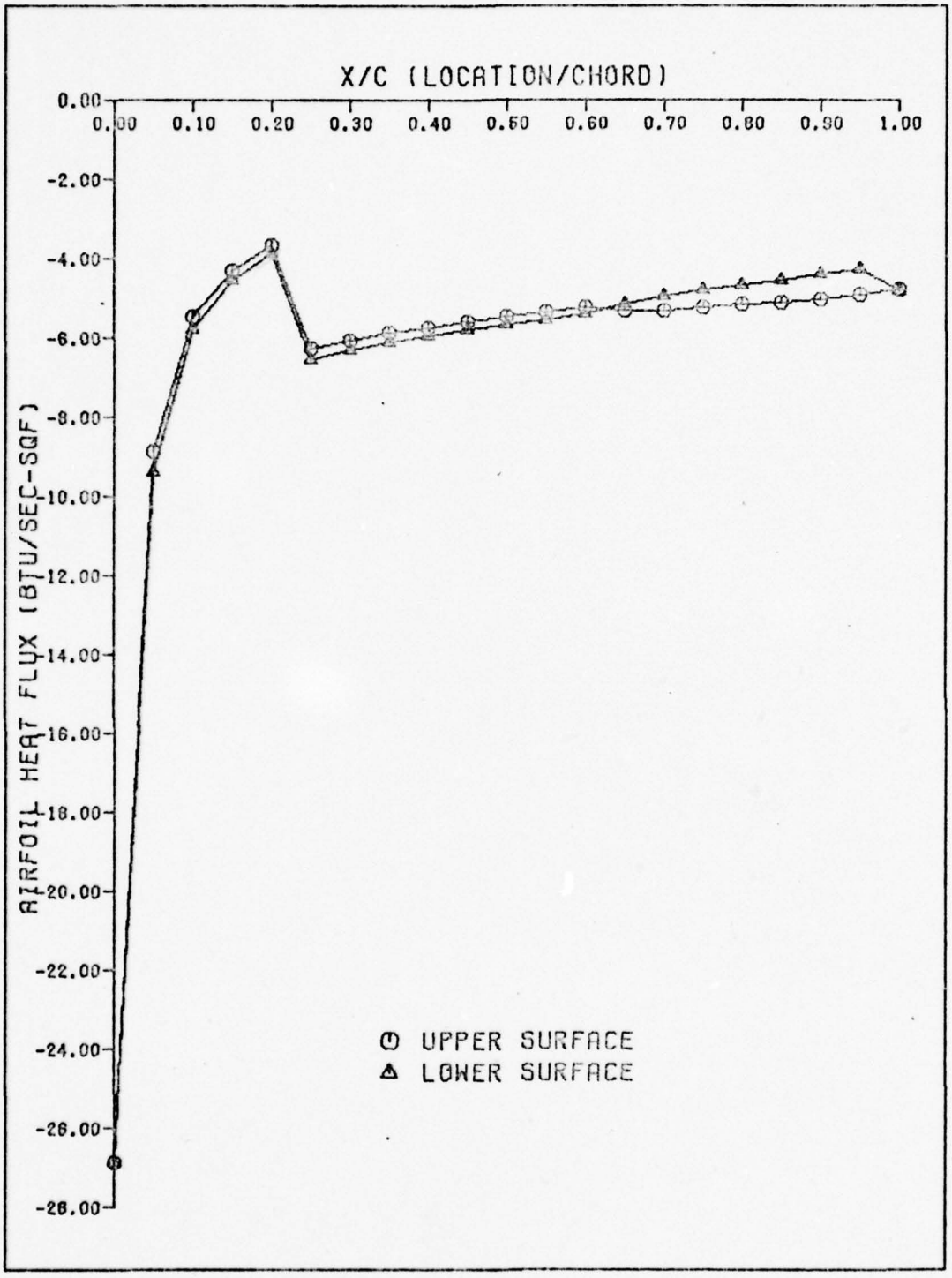

Fig. 4 Airfoil Heat Flux at the Design Condition
M=0.7, Re=1.673 x 10^6, T_w/T_∞ =0.620

Table I

Airfoil Local Properties at the Design Condition
$M=0.7$, $Re=1.673 \times 10^6$, $T_w/T_\infty = 0.620$

FREE STREAM CONDITIONS-
VEL= 813.052 MU= .370445E-06
P= 1330.439 TEMP RATIO= .620

XU(FT)	VEL(F/S)	RE AT EDGE	ST.NO.	H(BTU/S-SQF-R)	Q(BTU/SQF-S)
0.	0.	0.	0.	.1004E+00	-.2668E+02
.4633E-01	.1081E+04	.1737E+06	.3364E-02	.3833E-01	-.7095E+01
.8630E-01	.1094E+04	.3158E+06	.2087E-02	.2177E-01	-.5477E+01
.1240E+00	.1091E+04	.4555E+06	.1644E-02	.1722E-01	-.4330E+01
.1630E+00	.1087E+04	.5932E+06	.1438E-02	.1456E-01	-.3665E+01
.2010E+00	.1084E+04	.7340E+06	.1346E-02	.1401E-01	-.3293E+01
.2380E+00	.1079E+04	.8758E+06	.1295E-02	.1370E-01	-.3082E+01
.2750E+00	.1074E+04	.1011E+07	.1284E-02	.1356E-01	-.2997E+01
.3120E+00	.1070E+04	.1152E+07	.1272E-02	.1347E-01	-.2943E+01
.3500E+01	.1067E+04	.1294E+07	.1267E-02	.1345E-01	-.2916E+01
.3880E+00	.1063E+04	.1438E+07	.1263E-02	.1343E-01	-.2898E+01
.4250E+00	.1074E+04	.1582E+07	.1258E-02	.1341E-01	-.2886E+01
.4630E+00	.1084E+04	.1698E+07	.1255E-02	.1340E-01	-.2877E+01
.5000E+00	.1014E+04	.1847E+07	.1252E-02	.1339E-01	-.2870E+01
.5380E+00	.9606E+03	.1958E+07	.1249E-02	.1338E-01	-.2865E+01
.5750E+00	.9588E+03	.2104E+07	.1247E-02	.1338E-01	-.2861E+01
.6130E+00	.9586E+03	.2251E+07	.1246E-02	.1338E-01	-.2858E+01
.6510E+00	.9587E+03	.2398E+07	.1245E-02	.1338E-01	-.2856E+01
.6890E+00	.8947E+03	.2474E+07	.1243E-02	.1337E-01	-.2853E+01
.7280E+00	.8359E+03	.2537E+07	.1240E-02	.1334E-01	-.2842E+01
.7670E+00	.7995E+03	.2612E+07	.1236E-02	.1330E-01	-.2835E+01
XL(FT)	VEL(F/S)	RE AT EDGE	ST.NO.	H(BTU/S-SQF-R)	Q(BTU/SQF-S)
0.	0.	0.	0.	.1004E+00	-.2668E+02
.4330E-01	.8064E+03	.1737E+06	.3437E-02	.3847E-01	-.6990E+01
.8630E-01	.9648E+03	.3174E+06	.2103E-02	.2074E-01	-.4786E+01
.1240E+00	.9820E+03	.4588E+06	.1663E-02	.1732E-01	-.4572E+01
.1630E+00	.9766E+03	.5960E+06	.1407E-02	.1619E-01	-.3876E+01
.2010E+00	.9468E+03	.7346E+06	.1274E-02	.1554E-01	-.3550E+01
.2380E+00	.9270E+03	.8648E+06	.1255E-02	.1430E-01	-.6310E+01
.2750E+00	.9231E+03	.1002E+07	.2134E-02	.2351E-01	-.6107E+01
.3120E+00	.9270E+03	.1137E+07	.2126E-02	.2348E-01	-.5961E+01
.3490E+00	.9424E+03	.1275E+07	.2073E-02	.2336E-01	-.5793E+01
.3880E+00	.9366E+03	.1411E+07	.2023E-02	.2154E-01	-.5670E+01
.4250E+00	.9068E+03	.1541E+07	.1931E-02	.2137E-01	-.5558E+01
.4630E+00	.8677E+03	.1660E+07	.1860E-02	.2072E-01	-.5417E+01
.5000E+00	.7666E+03	.1771E+07	.1827E-02	.1964E-01	-.5150E+01
.5380E+00	.7222E+03	.1734E+07	.1915E-02	.1955E-01	-.4941E+01
.5750E+00	.7012E+03	.1810E+07	.1885E-02	.1826E-01	-.4805E+01
.6130E+00	.6954E+03	.1907E+07	.1850E-02	.1741E-01	-.4690E+01
.6510E+00	.6940E+03	.1979E+07	.1845E-02	.1728E-01	-.4554E+01
.6890E+00	.6612E+03	.2037E+07	.1825E-02	.1673E-01	-.4414E+01
.7310E+00	.6151E+03	.2058E+07	.1811E-02	.1617E-01	-.4271E+01
.7705E+00	.7095E+03	.2622E+07	.1783E-02	.1344E-01	-.4826E+01

TOTAL HEAT FLOW IN BTU/SEC IS -.1703E+02

As an obvious concession to the method discussed, a simple estimate was applied. The Fourier equation for heat conduction was approximated by

$$\dot{q}'' = -\frac{k\Delta T}{t} \qquad (12)$$

where t is the thickness normal to the airfoil surface. Equation 12 was used with the results of the convective heat transfer analysis. An average heat flux was found for the upper airfoil surface only since this was the surface of primary interest. This heat flux was computed by taking the mathematical average of the flux at each point excluding the stagnation point from Table I.

For the case of the airfoil, the maximum acceptable temperature difference through the surface was specified to be 3 F. The thickness, t, was assumed. Then a temperature difference was computed using the average heat flux. This temperature difference was compared to the limit to determine acceptability.

The minimum insulating end section thickness for the airfoil which was required to prevent the wind tunnel window from breaking or condensating moisture was determined by a heat flow balance. The cooling of the window caused by conduction in the model was equated to the heat convection to the wind tunnel window. The flow over the window was assumed to be fully developed turbulent duct flow. A temperature of 70 F was required to be maintained in the window glass. This heat balance was solved for the required thickness.

Selections of construction materials and material thicknesses were made using these estimates. The average heat flux on the upper surface of the airfoil was 5.451 B/sec-ft^2. Aluminum, which has a thermal conductivity of 0.03806 B/sec-ft^2-R/ft, was selected for the airfoil center section. A 0.187 in. thick surface of aluminum caused a temperature difference of 2.23 F when computed from Eq 12. Thus, the airfoil was designed with a constant thickness of 0.187 in. White oak which has a thermal conductivity of 1.38×10^{-5} B/sec-ft^2-R/ft was selected for the insulating end sections. A 0.0122 in. minimum thickness is required to keep the window at 70 F. However, due to structural considerations, the end sections were designed to be 0.813 in. thick.

Cooling System Design

The airfoil cooling system was designed to permit variation of the cooling ratio during the wind tunnel test. The system had to be capable of cooling the model to -113 F which corresponds to the cooling ratio of 0.620 and had to minimize temperature gradients in both the spanwise and chordwise directions.

Liquid nitrogen was selected as the coolant. This selection was based on the following properties (Ref 4:74) at one atmosphere of pressure:

$$T_{Boil} = -320 \text{ F}$$

$$\Delta i_{fg} = 85.9 \text{ B/lb}_m$$

$$\rho = 50.46 \text{ lb}_m/\text{ft}^3$$

The cooling system was designed to operate on liquid nitrogen only. The mass flow rate of liquid required to cool the airfoil at the design condition was estimated by

$$\dot{m} = Q/\Delta i_{fg} \tag{13}$$

where Q is the total heat transfer rate from Table I.

The inlet area required to carry the liquid was determined by assuming that the density was constant and that the average velocity of the fluid was 20 ft/sec. To ensure a safety factor in the cooling capacity, this inlet area was increased by 120 percent.

The airfoil is cooled by spraying liquid nitrogen on the inner walls of the model from nozzles. Most of the energy is absorbed by vaporization, and the resulting gas is expelled into the wind tunnel. The most complicated part of the cooling system design was locating and sizing these nozzles.

The cooling system design was based on the predicted total heat transfer rate and the heat flux distribution at the design condition. The total heat flow of 17.03 B/sec was used to approximate the mass flow of liquid nitrogen required. From Eq 13, this mass flow rate was 0.198 lb_m/sec. The inlet area to the airfoil which was computed and multiplied by the safety factor was 0.0622 in^2. The nozzles which are pipes of 1/8 in. nominal size were located as shown in Fig 5. This location was based on the heat flux distribution in Fig 4. The required inlet area was achieved by drilling the nozzles with a number 76 bit for a total of 198 holes. The holes were

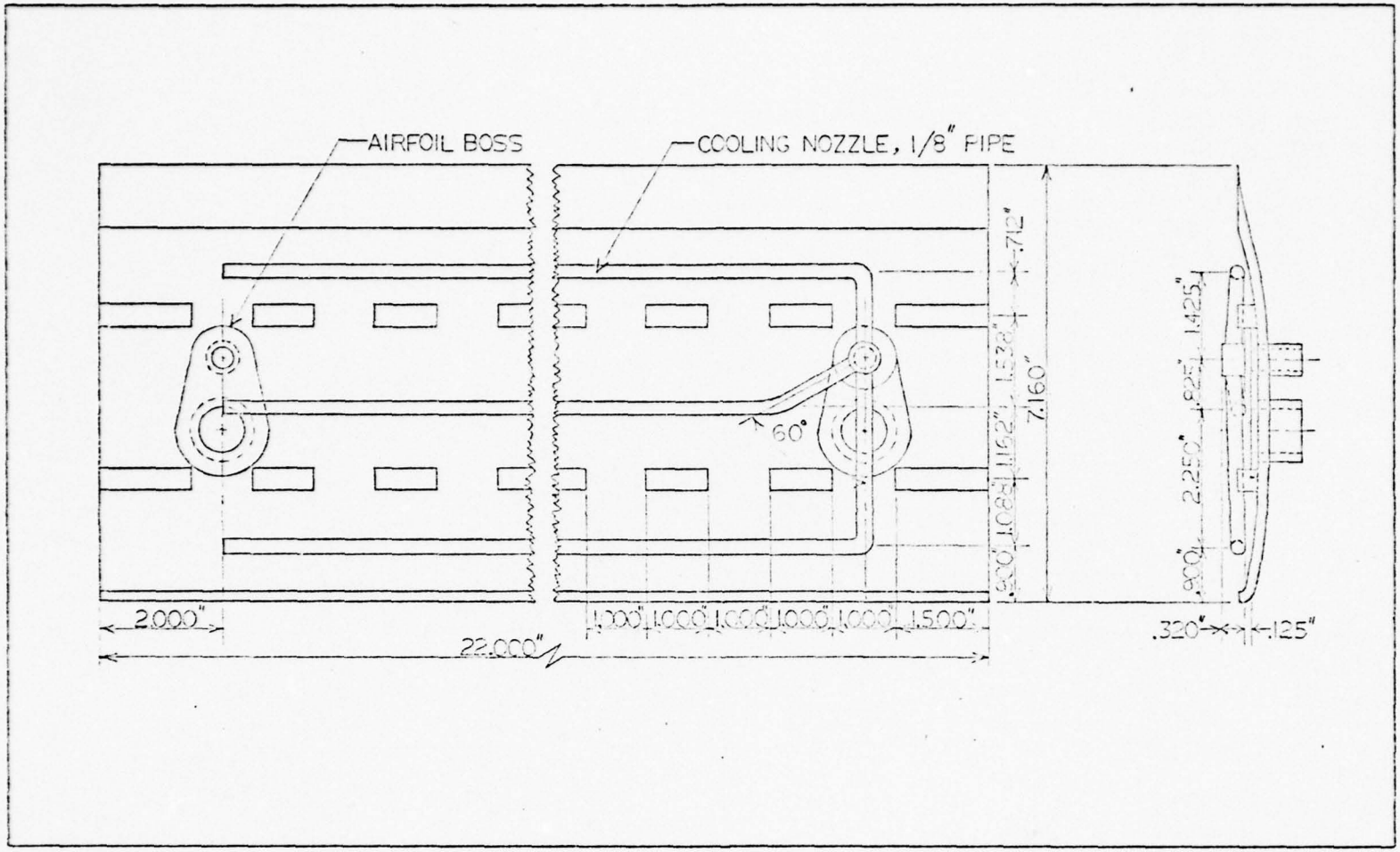

Fig. 5 Airfoil Lower Section with Cooling Nozzles and Airfoil Boss

distributed over the entire length of the nozzles with a larger number of holes in areas of high heat flux. Forty-four percent of the holes must be in the leading edge nozzle. The middle nozzle must contain 34 percent of the holes. Twenty-two percent of the holes must be in the trailing edge nozzle. The required exhaust area was 0.8648 in^2, which is 14 times the area of the inlet to ensure unrestricted flow.

The remainder of the system consisted of the liquid nitrogen supply source and connections through the mounting struts of the model. One strut contained the liquid nitrogen supply line. Both struts contained exhaust pipes for the nitrogen gas as illustrated in Fig 1. The nitrogen supply for the system consisted of a dewar of liquid nitrogen with insulation, a compressed nitrogen gas bottle at 2250 psi, and a pressure regulator. Regulated compressed gas pressurized the dewar to permit adjustment of the mass flow rate. Pressure relief values were used to prevent over pressurizing the model, piping, and dewar.

III. Airfoil Test Model Design

Aerodynamic Loads

Test loads on the airfoil and the mounting struts were predicted. Lift, drag, and pitching moment act on the airfoil. The only force acting on the symmetrical struts is drag. A small number of known experimental results for the DSMA 523 airfoil served as initial conditions for the computation. These known values, which were obtained from Ref 8, are the following:

$M = 0.82$

$Re_x = 3 \times 10^6$

$C_l = 0.51$

$C_d = 0.015$

C_p, Pressure distribution

The angle of attack and moment coefficient for the conditions were unknown. The problem was to find the force and moment coefficients for $M=0.7$ and $Re_x=1.673 \times 10^6$ at the zero angle of attack.

Angle of Attack. Equations were derived which relate the force and moment coefficients to the angle of attack and were used to determine the angle of attack for the known experimental conditions. The forces and moments that act on an airfoil are depicted in Fig 6.

The summation of forces in the x- and z- directions and the summation of the moments about the leading edge must be equal to zero to satisfy equilibrium. A summation of forces in the x- and z-direction using Fig 6 yields:

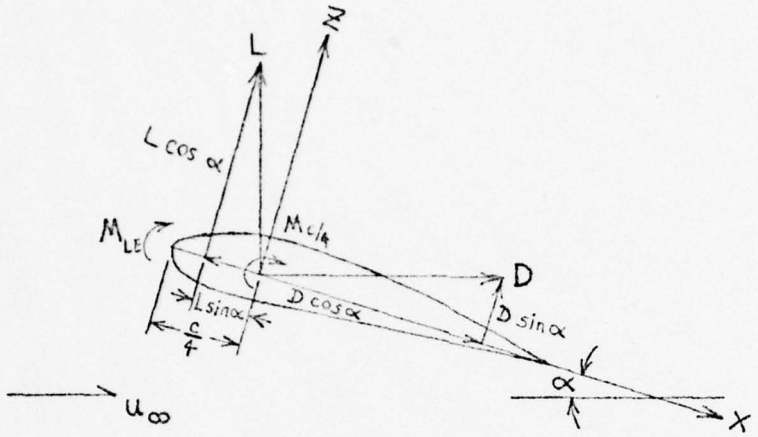

Fig. 6 Forces and Moments on a Typical Airfoil Section

$$C_d \cos\alpha - C_\ell \sin\alpha = 0 \tag{14}$$

$$C_d \sin\alpha + C_\ell \cos\alpha = 0 \tag{15}$$

Finally, summation of moments about the leading edge gives

$$C_{m_{c/4}} = \frac{C_d}{4}\sin\alpha + \frac{C_\ell}{4}\cos\alpha \tag{16}$$

Equation 14 was solved for the angle of attack to obtain

$$\alpha = \tan^{-1}(C_d/C_\ell) \tag{17}$$

The angle of attack was determined to be $\alpha = 1.6^\circ$ since C_d and

C_l were known.

Determination of Quarter Chord Pitching Moment Coefficient. Using the plot of pressure distribution of C_l=0.51, the moment coefficient about the quarter chord point was determined to be $C_{m\ c/4}$=0.123. Details of the method used can be found in Ref 7:83-85 and consisted of numerically integrating the pressure distribution for directions both normal and perpendicular to the chord. Then, an appropriate coordinate transformation was performed. This result was verified by the solution of Eq 16 with very close agreement.

Determination of Theoretical Coefficients. The previously derived equations and results were used to find the theoretical coefficients at the zero angle of attack. It was assumed that the drag coefficient which was presented contained only pressure drag. Thus, it was necessary to add skin friction drag. The skin friction coefficient was calculated using the method of Van Driest (Ref 15) which computes the compressible, turbulent skin friction coefficient for a flat plate as a function of heat transfer. The adiabatic condition was assumed. The resulting total drag coefficient was 0.034.

The ideal lift curve slope for a flat plate was assumed to apply, and the following relation was derived:

$$C_l - C_{l_i} = 2\pi(\alpha - \alpha_i) \tag{18}$$

where "i" denotes initial conditions. Equations 14, 16, and 18 define the relationship between the coefficients and angle of attack.

Determination of Forces and Moment. The forces and moment on the airfoil could be computed when the dynamic pressure and the wing planform area were specified. The dynamic pressure was expressed as

$$q = \gamma M_\infty^2 P_\infty / 2 \tag{19}$$

where $\gamma = 1.4$ for air and M_∞ and P_∞ were defined for the design condition. The airfoil chord was specified to be 0.750 ft and the span was specified to be 2.0 ft. Thus, the planform area was 1.50 ft^2.

Strut Drag. Only the vertical portion of the strut was considered since the horizontal portion in the wake of the vertical strut was assumed to contribute negligibly to the total drag. Since the struts were symmetric and parallel to the flow, the only force that occurred was drag. The Reynolds number was 487,800 for the 2.625 in. chord of the strut. The thickness ratio, t/c, was 0.57 or 57 percent. Based on a critical Reynolds number of 110,000 for an approximately 50 percent thick bluff body as suggested by Hoerner (Ref 6:6-5), the location of transition was 0.0493 ft. The laminar and turbulent skin friction coefficients were computed by

$$C_{f_{Lam}} = 1.328/\sqrt{Re_x}$$

and

$$C_{f_{Tur}} = 0.074/Re_x^{1/5}$$

A weighted mean value based on length was found for the skin

friction coefficient. The total drag coefficient was estimated by (Ref 6:6-9)

$$C_d/C_f = 4 + 2\,c/t + 120(t/c)^3 \qquad (20)$$

where C_d is based on frontal area and t/c is the thickness to chord ratio.

Results. At M=0.7 and $\alpha=0^\circ$, the aerodynamic loads which were computed from the theoretical coefficients for the airfoil are the following:

$$L = 299.0\ lb_f$$
$$D = 12.9\ lb_f$$
$$M = 56.0\ ft\text{-}lb_f$$

The total strut drag was 14.5 lb_f. The theoretical design coefficients for lift and drag were 0.440 and 0.019, respectively.

Stress Analysis

A stress analysis was performed on the entire airfoil model and the wind tunnel mounting struts to ensure that the model was capable of sustaining the loads that were predicted for the design condition. Specifically, the safety factor was required to be a minimum of 4. Simplifying assumptions reduced the analysis to an application of beam bending theory. The model and mount were divided into major components (Fig 1): the airfoil, airfoil mounting boss, wind tunnel mounting struts, and strut mounting plates. The procedures used were applied to all components.

Assumptions. Due to the two-dimensional flow, the spanwise force and moment distributions on the airfoil model were uniform. The chordwise force distribution was assumed to be such that the net result acted at the quarter chord point of each section. This assumption is normal for subsonic flow. The reaction of the mounting struts to the air loads was assumed to occur at the center of the strut exhaust pipe and to act as a point force concurrent with the lift force. The airfoil was assumed to act as a simple beam with a uniform load where the struts supported no spanwise moments. To find the torsional stress due to the aerodynamic moment, the airfoil was assumed to be an elliptical shell with the major axis equal to the chord and the minor axis equal to the maximum thickness of the airfoil. The cross-sectional area and moment of inertia about the axis normal to the chord were forced to be the same as for the airfoil.

Due to model symmetry, the loads were divided equally to each strut. Since the airfoil and wall acted as end plates, the flow over the strut was assumed to be two-dimensional and to create a uniform drag force. The forces and moment on the strut were assumed to occur at the center of the exhaust pipe which is located at 28 percent chord. The analysis of the strut was divided into the vertical portion and horizontal portion, where both were assumed to act as cantilever beams with concentrated loads. This assumption was valid if deflections at the fixed ends were negligible. All loads were assumed to be carried by the exhaust pipe for the vertical

portion and by the shape labeled Section A-A in Fig 7 for the horizontal portion.

The airfoil mounting boss and boss plate were designed to connect the airfoil to the strut and are illustrated in Fig 8 and Fig 9, respectively. Any vertical translation of the drag force was assumed negligible since this force is small and the distance of translation was less than one inch. An equivalent couple acting on the centerline was assumed to replace the aerodynamic moment.

The strut mounting plate was designed to fasten the strut to the wind tunnel wall. The forces that acted on this plate were assumed to behave as point forces acting at the centroid of the four mounting bolts which was 0.375 in. from the location used to compute the stresses on the horizontal portion of the strut. The forces and moment on the horizontal strut were assumed to act on the plate since translation over the small distance was negligible.

General Procedures. Moments of inertia and centroids of area were computed for the cross-section of each component from a method of built-up elements. Any complicated section shape was divided into simple elemental areas. Then, the following formulas were used:

$$A=\sum_{i=1}^{N} a_i \tag{21}$$

$$C_x=\frac{1}{A}\sum_{i=1}^{N} x_i a_i \tag{22}$$

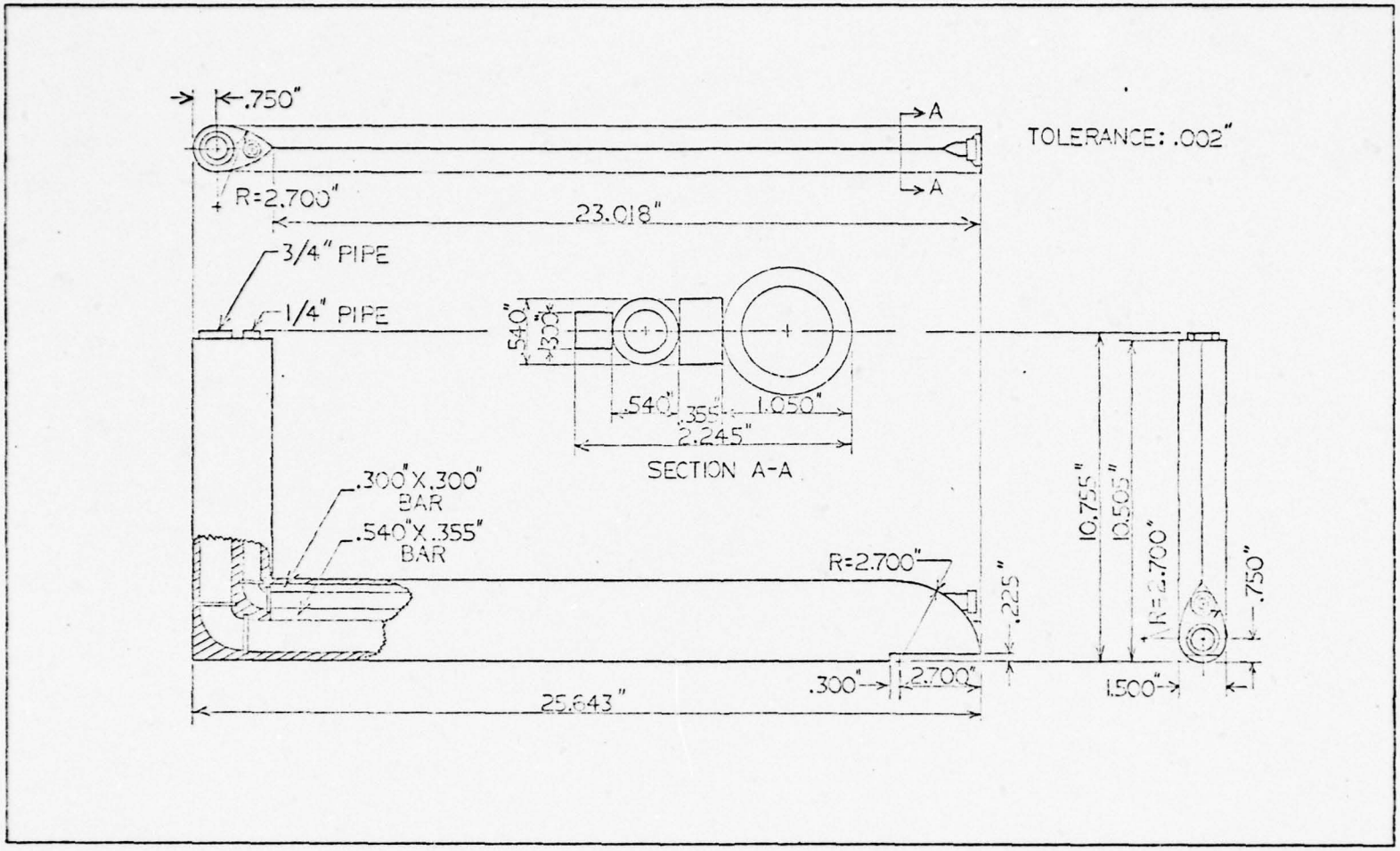

Fig. 7 Mounting Strut

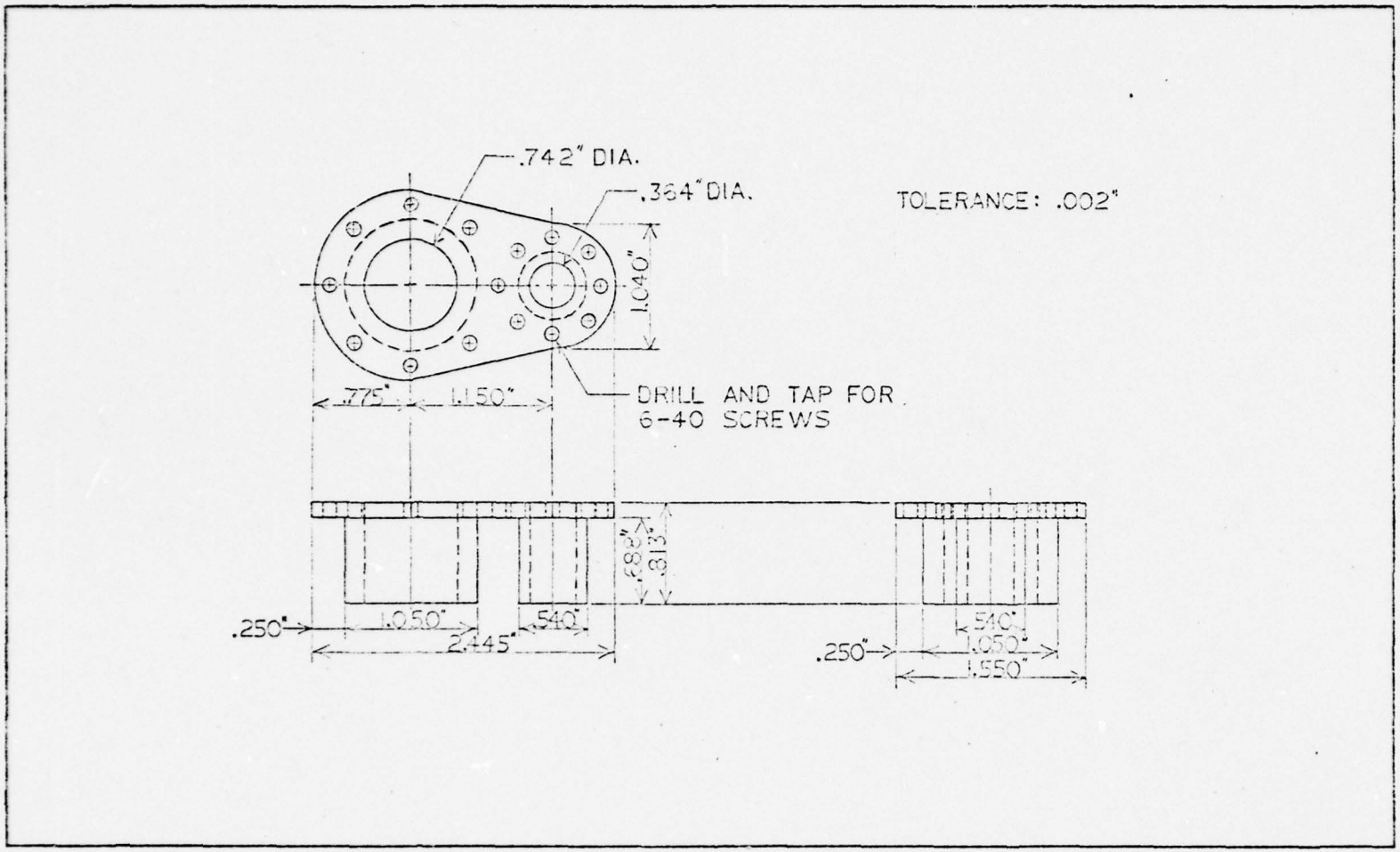

Fig. 8 Airfoil Mounting Boss

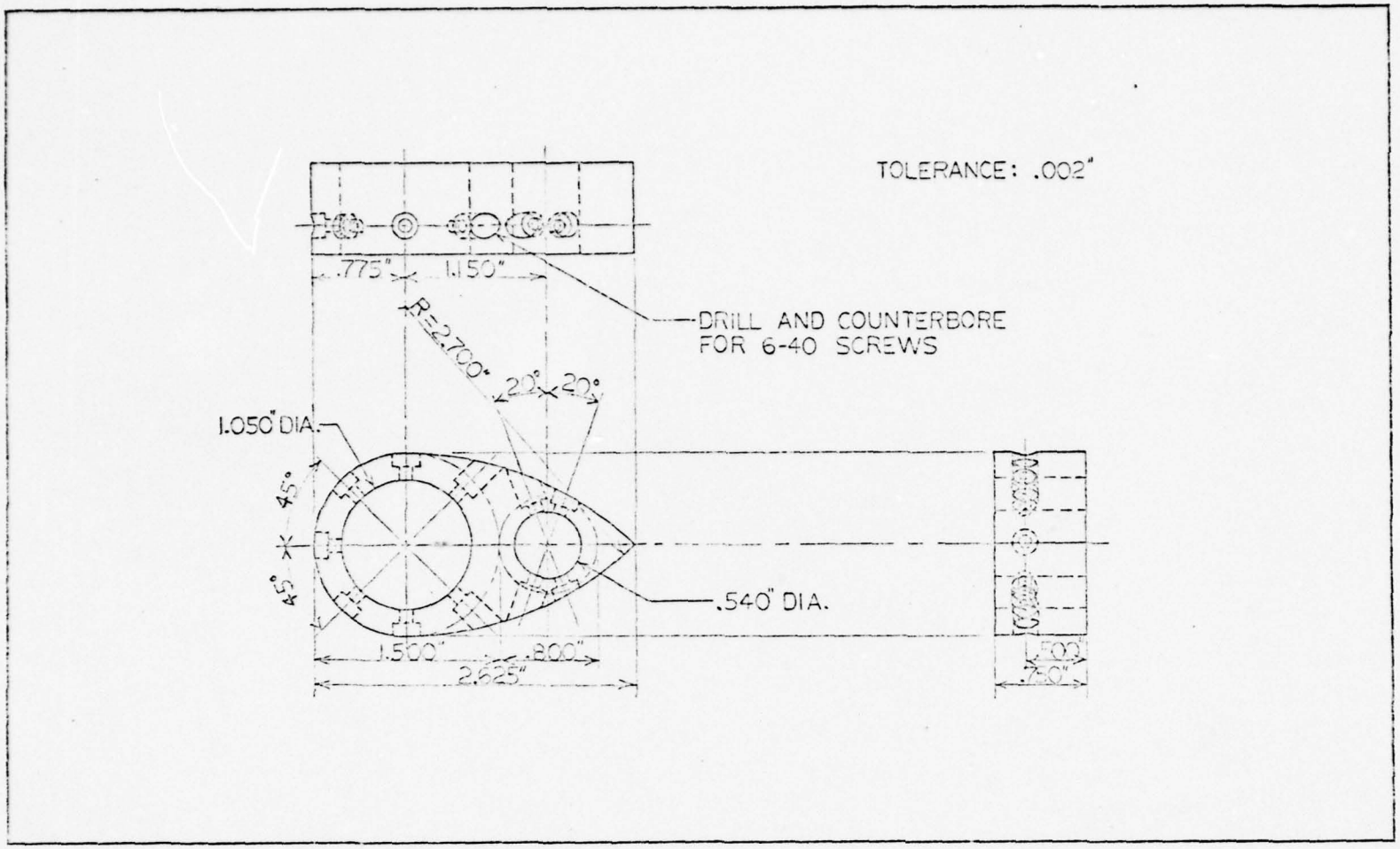

Fig. 9 Strut Boss Plate

$$C_y = \frac{1}{A} \sum_{i=1}^{N} y_i a_i \tag{23}$$

$$I_x = \sum_{i=1}^{N} y_i^2 a_i \tag{24}$$

$$I_y = \sum_{i=1}^{N} x_i^2 a_i \tag{25}$$

$$I_{xy} = \sum_{i=1}^{N} x_i y_i a_i \tag{26}$$

If the moments of inertia were found about a set of axes at any point other than the centroid of the cross-section, then the parallel axis theorem was used to obtain the moments of inertia about the centroidal axes.

The material selection was based on the thermal and structural properties. If after the stress analysis the safety factor was less than 4, a new material with greater strength was selected. The particular structural properties of interest in the analysis were the yield strengths and ultimate strengths under tension, compression, and shear. These were used to compare with the predicted design loads and to define the safety factor.

Each component was isolated during the analysis. An equivalent force system had to be described which produced the same effect on that component as the reaction to the adjacent component. The equivalent system was obtained by moving forces along their lines of action or by parallel translation which required the introduction of a couple. Some uniformly

distributed forces were replaced by a point force acting at the center of the distributed load area.

Each component was examined to define critical points which were suspected of sustaining large stress concentrations due to changes in cross-sectional area, curvature, or distance from the applied load. The critical points were the only locations where the maximum stresses and safety factors were computed.

Special considerations were necessary to compute the stress on the airfoil and the strut. The shear stress due to torsion on the airfoil was computed by a method detailed in Ref 17:53. This shear stress is given by

$$\tau = \frac{2T}{\pi a_1 b_1^2 \left[(1+q)^4 - 1 \right]} \tag{27}$$

where

$$q = \frac{a - a_1}{a_1} = \frac{b - b_1}{b_1}$$

and the subscript, 1, denotes the axial length measured to the inside of the shell. The insulating end sections of the airfoil which were assumed to be a solid elliptical shaft required the use of

$$\tau = 2T/\pi a b^2 \qquad (\text{for } a > b) \tag{28}$$

The mounting struts had a sharp curvature which caused stress concentration. Oberg (Ref 11:433) presented a method to correct for curvature effects. This correction factor was a function of the radius of curvature.

The component was modeled as a simple beam of constant cross-section. Vidosic (Ref 17:31-34) had compiled a table of solutions for the reactions, moments, and shear at any point on a uniform beam for a variety of conditions. A solution was selected from this table which matched the modeled component and equivalent force system.

To find the normal stress due to the bending moment, the flexure formula,

$$\sigma = Mc/I \tag{29}$$

was used. The stress due to each of the forces or moment was computed separately.

The resulting normal stresses from each force and moment at a point were combined by vector addition. Shear stresses were combined in the same manner. The remaining normal and shear stresses were combined to find the maximum stresses at the point. The formulas used from Ref 11:421 to combine the stresses were the following:

$$\sigma_{max} = \frac{\sigma_x + \sigma_y}{2} + \sqrt{\left(\frac{\sigma_x - \sigma_y}{2}\right)^2 + \tau_{xy}^2} \tag{30}$$

$$\tau_{max} = \sqrt{\left(\frac{\sigma_x - \sigma_y}{2}\right)^2 + \tau_{xy}^2} \tag{31}$$

The maximum stresses were compared to the yield and ultimate strengths of the material in the form of a safety ratio, SR. The safety ratios were combined by

$$FS = \frac{1}{\sqrt{SR_\sigma^2 + SR_\tau^2}} \qquad (32)$$

to produce one safety factor for the yield limit and one for the ultimate limit.

Results. The minimum yield safety factor of 7.4 on the airfoil occurred at mid-span where the maximum normal stress was 3298 psi, and the maximum shear stress was 2442 psi. On the strut, the minimum ultimate safety factor was 6.3 at the top of the horizontal portion which was 23.973 in. from the leading edge where the maximum normal stress was 9039 psi. On the mounting boss, the mounting screws had the minimum ultimate safety factor of 13.3 where the maximum stress was 4102 psi. On the strut mounting plate, the mounting bolts had the minimum ultimate safety factor of 4.4 where the maximum normal stress was 1032 psi, and the maximum shear stress was 7580 psi. A complete listing of the stresses and safety factors at the critical points is included in Appendix C.

Instrumentation

Thermocouples, located internal to the model, were the only instrumentation selected for use in the wind tunnel. Instrumentation which was external to the model could not be used due to a wind tunnel blockage problem that was caused by the model frontal area. Additional internal instrumentation could not be used since the space inside the model was very limited.

The purpose of the thermocouples was to determine the airfoil surface temperature at selected points which would indicate any strong temperature gradients that might influence transition, establish the cooling ratio used for that particular test run, and serve as a data base to be used with holography to obtain quantitative results. The thermocouples were needed primarily on the upper airfoil surface where the boundary layer transition would be investigated. The following list of desired characteristics was devised to select the proper thermocouple for this application:

1. Be very compact in size
2. Be locally produced to meet specifications
3. Useful range of -300 F to 200 F
4. Error range of ± 2% maximum
5. Short time constant for quick response

Copper-constantan thermocouples were selected to instrument the model. This type of thermocouple was recommended in Ref 12 for low temperature application due to the homogeneity of the metal. The thermocouples were located at mid-span of the airfoil. Figure 10 shows the location of the 8 thermocouples along the upper surface.

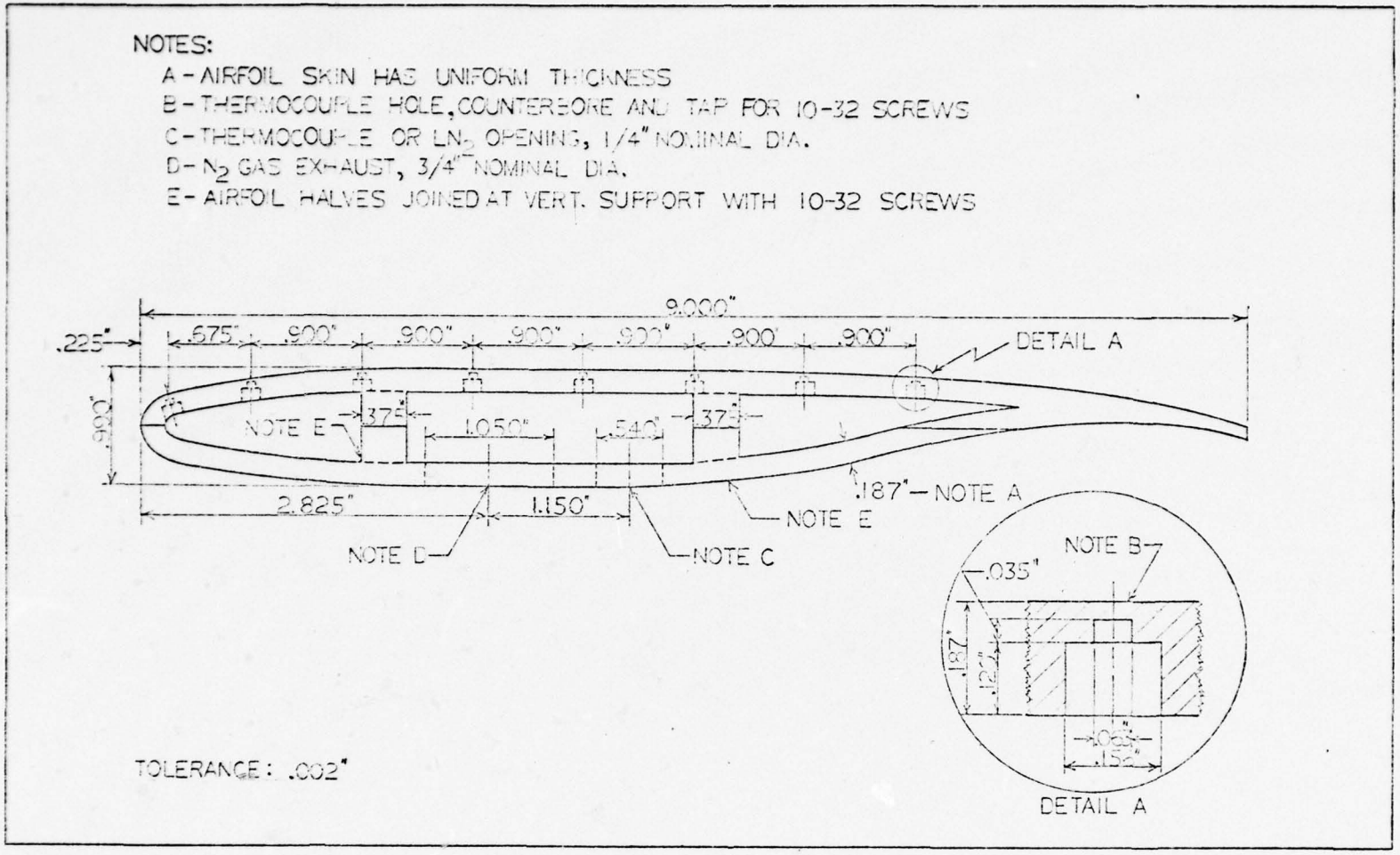

Fig. 10 Airfoil Model Cross Section

IV. Proposed Test Procedures

Test Conditions

The wind tunnel test conditions to be used were established. Parameters of interest in the test, Mach number, Reynolds number, and cooling ratio, were specified to limit the number of test runs and to give a representative sample of conditions. The Trisonic wind tunnel stagnation temperature was considered to be 100 F. Freestream viscosity, which is a function of the specified stagnation temperature and Mach number, was computed from Sutherland's equation (Eq 10). The only parameter left to be computed was the stagnation pressure.

The relationship between the stagnation pressure, Reynolds number, and Mach number was derived by substituting the definition of Mach number and the perfect gas law into the Reynolds number definition. After introducing the isentropic relationships for pressure and temperature, the expression was solved for the stagnation pressure with the following results:

$$P_o = \frac{Re_\infty \mu_\infty}{c M_\infty} \sqrt{\frac{RT_o}{\gamma}} \left(1 + \frac{\gamma - 1}{2} M_\infty^2\right)^{\frac{\gamma+1}{2(\gamma-1)}} \qquad (33)$$

Equation 33 was used to establish the proposed test conditions which appear in Table II.

Test Equipment

Pulse laser holography and schlieren were considered

Table II

Wind Tunnel Test Parameters for $T_o = 560$ R

M	$\mu_\infty \times 10^6$ (lb-sec/ft^2)	P_o(psia) for Re=0.923 x 10^6	P_o(psia) for Re=1.673 x 10^6
0.3	0.39279	9.972	18.080
0.5	0.38358	6.412	11.624
0.7	0.37049	5.058	9.170

for use during the test. Optical methods of data collection were necessary due to the high blockage in the wind tunnel. The selection of equipment was based on the information obtained from Ref 10 for the schlieren method and Ref 5 for the holographic method. Pulse laser holography was selected as the primary method of recording the boundary layer transition.

The schlieren method would provide a recording of the density gradients in the flow field. The boundary layer transition would not appear as a point but would appear as a thickening of the boundary layer over a small region. The disadvantages of this method were that the results would only be qualitative and that the transition would be difficult to detect if the density gradients were not strong.

The pulse laser holography method had several advantages. Holography produces a hologram which could be used later to reconstruct a shadowgraph, schlieren, or interfero-

gram. Qualitative results could be viewed in different forms to select the best recording of transition. In additon, the hologram could be magnified to help locate transition. An interferogram produced by holography could be used to provide quantitative results of the density gradients. With the density and temperature distributions available, the pressure distribution could be found.

V. Heat Transfer for Test Conditions

There were two problems with the design process at this point. First, the results of Boehman, Fig 2, had not been incorporated into the program, CONHEAT. A critical Reynolds number of 0.5×10^6, which did not change as a function of the cooling ratio, had been used. Second, the pressure distribution used was for a Mach number of 0.82 since it was the only one available for the DSMA 523 airfoil. The model design was completed by necessity with this data.

Test Data. Through a cooperative test program with NASA Ames Research Center, McDonnell Douglas Research Laboratories had completed pressure measurements on the DSMA 523 airfoil at a Mach number of 0.7 and Reynolds number of 2.0×10^6. Spaid (Ref 14) obtained special permission from NASA and the McDonnell Douglas Corporation for the data to be used in this study.

The new pressure distribution was incorporated into CONHEAT along with the variation of the critical Reynolds number with cooling ratio. Careful observation of Fig 2 shows that the critical Reynolds number may not be reached for the given freestream Reynolds numbers and cooling ratios below 0.824. Therefore, the range of desired cooling ratios was changed to 1.000 through 0.824.

Forced Convection Predictions. As a result of using the new test data with CONHEAT, predictions of the heat transfer for several cooling ratios were obtained at M=0.7. The

variation of heat flux followed the same pattern as the design condition flux; however, the magnitude of flux decreased and the location of transition moved forward for each increasing cooling ratio. As can be seen in Fig 11, the transition to turbulent flow did not occur at all for $Re=0.923 \times 10^6$ and $T_w/T_\infty = 0.824$. The remaining heat flux predictions can be found in Appendix B.

Due to the differences in design and test data, a comparison of the total heat transfer rate for these two conditions was made to ensure the capacity of the cooling system was adequate for the test. This comparison (Fig 12) showed that the required cooling for both freestream Reynolds numbers was less than the design values at the same cooling ratio.

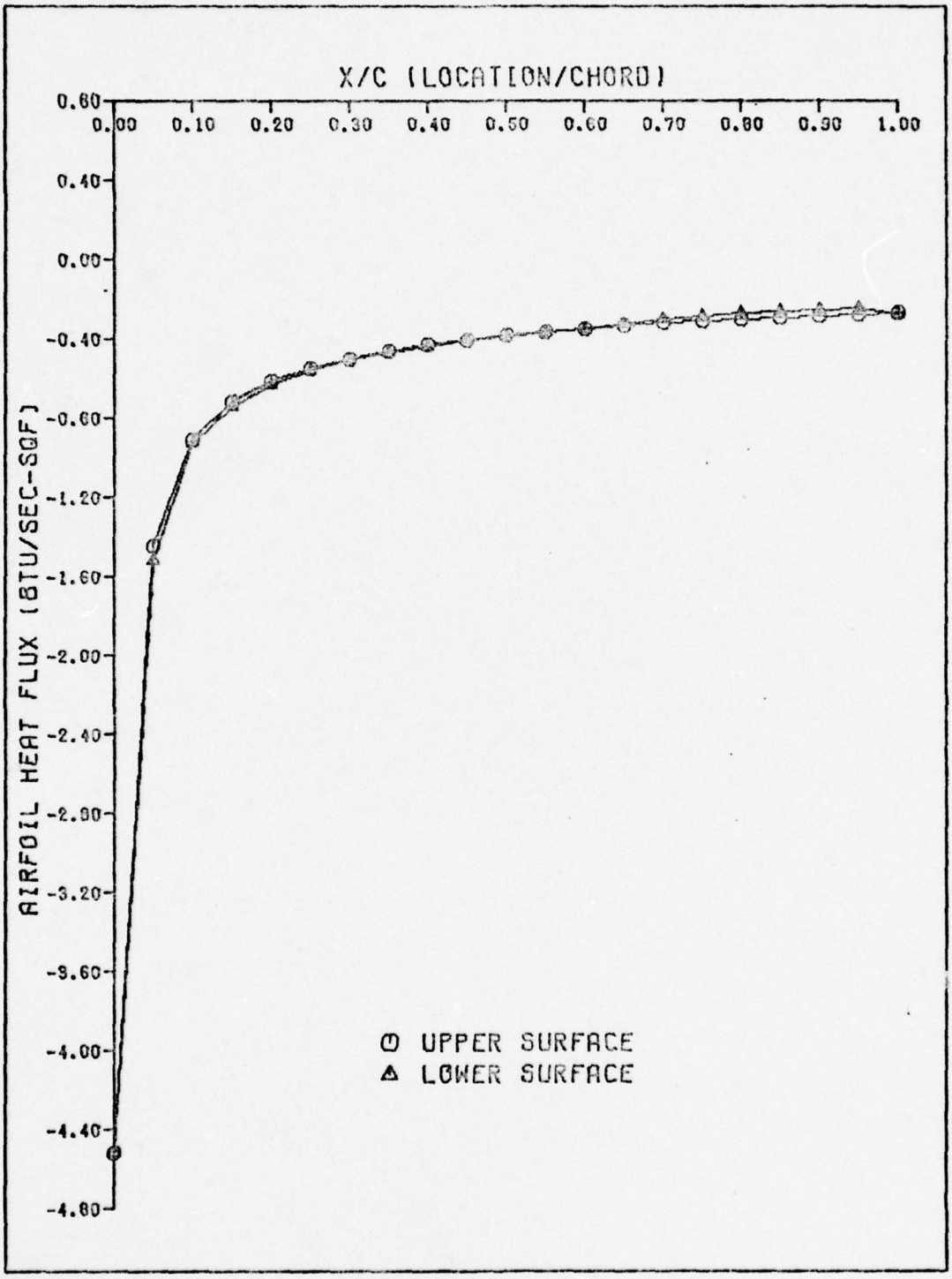

Fig. 11 Airfoil Heat Flux at M=0.7, Re=0.923 x 10^6, and T_w/T_∞ =0.824

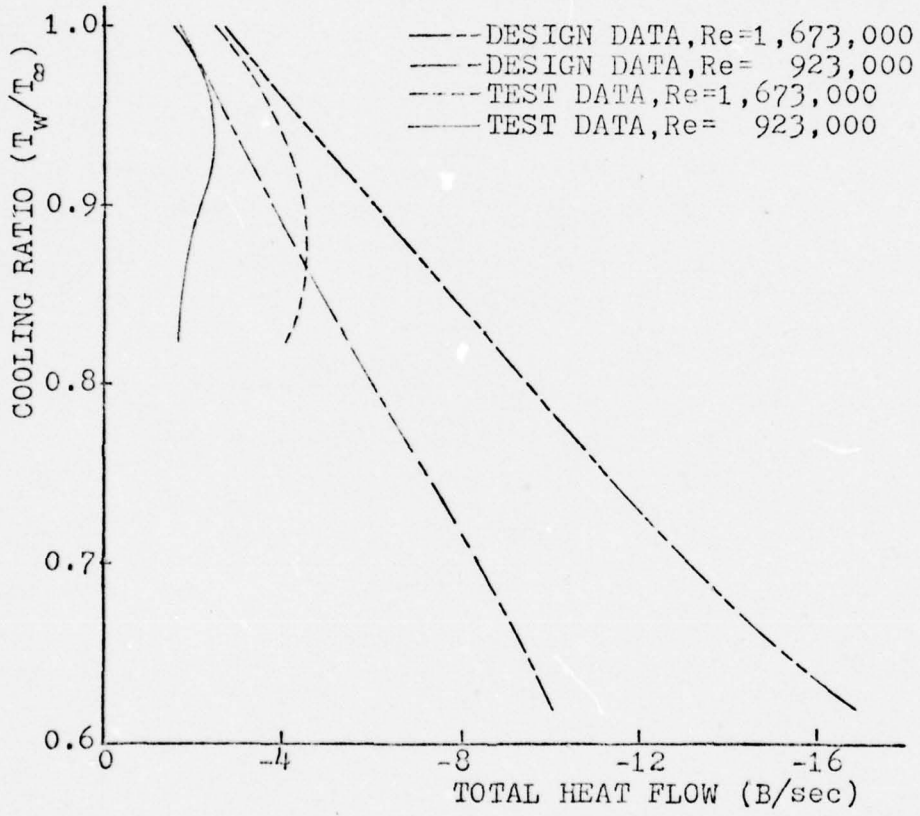

Fig. 12 Total Heat Flow as a Function of Cooling at M=0.7

VI. Design Summary and Recommendations

The following items summarize the capability of the airfoil test model:

1. The angle of attack which is not adjustable is $\alpha=0^{\circ}$.
2. The maximum allowable aerodynamic loads occur at M=0.7.
3. The maximum cooling capacity is 17.03 B/sec.
4. The maximum mass flow rate of coolant is $\dot{m}=0.198\ lb_m/sec$.
5. The maximum temperature gradient in the model is 2.23 F.
6. The maximum cooling experienced by the wind tunnel window is 0.004 B/sec.
7. The lowest safety factor which occurs at the strut mounting bolts is 4.4.

The first four recommendations are concerned with the testing of the airfoil model. The remaining recommendations propose further investigations. These recommendations are:

1. A bench check of the model cooling system and thermocouples should be made prior to the test.
2. Ensure the wind tunnel is dry as possible to prevent frost formation.
3. Compare the total heat flow for the experiment with predicted values by measuring the mass flow rate of coolant.

4. Compare the experimental results with the theoretical results from Ref 2.
5. Further experimental investigation of the cooling effects on transition should be conducted with a flat plate to eliminate pressure gradients.
6. Further experimental investigation of the cooling effects on transition should be conducted in a three-dimensional flow.

Bibliography

1. Ambrok, G. S. "Approximate Solution of Equations for the Thermal Boundary Layer with Variations in Boundary Layer Structure." Soviet Physics- Technical Physics, 2: 1979 (1957).

2. Boehman, L. I. and M. G. Mariscalco. The Stability of Highly Cooled Compressible Laminar Boundary Layers. AFFDL-TR-76-148. Wright-Patterson Air Force Base, Ohio: Air Force Flight Dynamics Laboratory, 1976.

3. Boison, J. C. "Highly Cooled Boundary Layer Transition Data in a Shock Tube." Modern Developments in Shock Tube Research. Japan: Proceedings of the Tenth International Shock Tube Symposium, 127 - 140, 1975.

4. Bolz, R. E. and G. L. Tuve. Handbook of Tables for Applied Engineering Science. Cleveland, Ohio: Chemical Rubber Co., 1970.

5. Havener, A. G. A Users Guide on Pulse Laser Holography for Wind Tunnel Testing. ARL TR 75-0213. Wright-Patterson Air Force Base, Ohio: Aerospace Research Laboratories, 1975.

6. Hoerner, S. F. Fluid- Dynamic Drag. Great Britain: By author, 1965.

7. Houghton, E. L. and A. E. Brock. Aerodynamics for Engineering Students (Second Edition). London: Edward Arnold (Publishers) Ltd, 1970.

8. Hurley, F. X., F. W. Spaid, F. W. Roos, L. S. Stivers, Jr., and A. Bandettini. "Supercritical Airfoil Flowfield Measurements." Journal of Aircraft, 12: 737 - 744 (September 1975).

9. Kays, W. M. Convective Heat and Mass Transfer. New York: McGraw - Hill Book Co., 1966.

10. Ladenburg, R. W., B. Lewis, R. N. Pease, and H. S. Taylor. Physical Measurements in Gas Dynamics and Combustion. Vol. IX: High Speed Aerodynamics and Jet Propulsion. Princeton, New Jersey: Princeton University Press, 1954.

11. Oberg, E., F. D. Jones, and H. L. Horton. Machinery's Handbook (Twentieth Edition). New York: Industrial Press, Inc., 1975.

12. Omega Engineering Company. The Omega Temperature Measurement Handbook. Stanford, Conn.: Omega Engineering Co., 1973.

13. Smith, A. G. and D. B. Spalding. "Heat Transfer in a Laminar Boundary Layer with Constant Fluid Properties and Constant Wall Temperature." Journal of the Royal Aeronautical Society, 62: 60 (January 1958).

14. Spaid, F. W. Personal Communication. Saint Louis, Missouri: McDonnell Douglas Corporation, 2 August 1977.

15. Van Driest, E. R. "Turbulent Boundary Layer in Compressible Flow." Journal of the Aeronautical Sciences, 18: 145 - 160 (1951).

16. Van Driest, E. R. and J. C. Boison. "Experiments on Boundary Layer Transition at Supersonic Speeds." Journal of the Aeronautical Sciences, 24: 885 - 899 (December 1957).

17. Vidosic, J. P. "Mechanics of Materials." Standard Handbook for Mechanical Engineers (Seventh Edition). Theodore Baumeister, Editor. New York: McGraw - Hill Book Co., 1967.

Appendix A

Computer Program for Boundary Layer Convection Study

The computer program called CONHEAT implemented the theory and program logic that were discussed in Section II to perform the convective heat transfer analysis. To use this program effectively, the format for input and output and definitions of parameters must be known. A listing of the complete program has been included in this appendix.

Input Format and Parameters

Two methods were used to input data. One method was the data statement, and the other was standard data cards. The data statement is part of the main program and was used for constants and variables which were seldom changed. Data cards were used for information which was generally changed or for variables which had to be redefined during a single execution of the program.

Five data statements were used. The data statement assigns values to variables and arrays. The word "DATA" may be followed by any number of variables with the value of each enclosed with slash marks. The first data statement defined constants and geometry of the model as follows:

GO - Newton's constant, g_o=32.174 lb_m-ft/lb_f-sec^2

R - Gas constant for air, R=1716 ft^2/sec^2-R

CJ - Mechanical to thermal energy conversion factor, J=778.16 ft-lb_f/B

CSH- Specific heat at constant pressure, C_p=0.24 B/lb_m-R

PR - Prandtl number for air, Pr=0.7

C - Airfoil chord in feet, c=0.75 ft

B - Airfoil span in feet, b=1.83 ft

RA - Leading edge radius in feet, r=0.025 ft

TIN- Freestream temperature, T_∞ =559.67 R

The second data statement defined the distance between pressure coefficient locations on the upper surface in the surface coordinate system. XU means the x-distance on the upper surface. All 21 points must be included. The values in this array are separated by commas. The following is an example:

DATA XU/0., .048, .086, ..., .770/

The third data statement has the same form as the second statement. It defines the x-distance on the lower surface, XL. The fourth data statement lists the pressure coefficients for the upper surface, CPU. The form is the same as the second statement. The fifth data statement lists the pressure coefficients on the lower surface, CPL.

The three read statements in the program are unformated to simplify use. This requires the data card to list the decimal values of the variables separated by commas and in the order that appears on the read statement. The first data card must contain the following:

UIN - Freestream velocity in ft/sec, u_∞

MUIN- Freestream viscosity in lb_f-sec/ft^2, μ_∞

PIN - Freestream pressure in lb_f/ft^2, P_∞

An example of this card is the following:

813.052, .0000037049, 728.048

The numbers start in column 1 of the card. There must be at least one card of this type. The second card indicates the number of cooling ratios to be read, NTR. The value on the second card must be a positive integer. The third data card lists the following:

TR - Cooling ratio, T_w/T_∞

REC - Critical Reynolds number corresponding to the value of TR of Fig 2

The total number of the third type of cards must equal the integer on the second card. If more than one set of free-stream conditions is specified, then all three types of cards must be repeated.

Output Format

Two types of output are obtained from the program. One type is a plot of the local heat flux, $\dot{q}''_w$, as a function of location along the chordline for the upper and lower surfaces. Examples of the plot appear in Appendix B. The second type of output is a table. The table includes freestream conditions, local values of properties, and the total rate of heat transfer. The local values of properties at each point include location, velocity, Reynolds number, Stanton number, convective conductance, and heat flux. An example of this table appears in Appendix B, Table III.

```
      PROGRAM CONHEAT(INPUT=/80,OUTPUT=/132,PLOT)
C*****************************************************************
C*   THIS PROGRAM ANALYZES FORCED CONVECTIVE HEAT TRANSFER IN THE BOUN- *
C*    DARY LAYER OF ANY AIRFOIL IF GIVEN THE FREE STREAM CONDITIONS AND *
C*    THE PRESSURE DISTRIBUTION ON THE SURFACE.                         *
C*   THE PROGRAM USES ECKERTS TEMP. TO ESTIMATE B.L. CONDITIONS AND COM-*
C*    PUTES THE LAMINAR AND TURBULENT STANTON NO.                       *
C*   STANTON NO. IS SOLVED FOR HEAT TRANSFER COEFF. W/ INTEGRATION BY   *
C*    TRAPEZOIDAL RULE.                                                 *
C*   LOCAL HEAT FLUX IS INTEGRATED TO GET TOTAL HEAT TRANSFER.         *
C*                                                                     *
C*   DEFINITION OF TERMS USED IN INPUT/OUTPUT-                         *
C*         TW - WALL TEMP (DEG RANKIN)                                 *
C*         PR - PRANDTL NO.                                            *
C*        ROI - FREE STREAM DENSITY (SLUGS/CUBIC FT)                   *
C*        TIN - FREE STREAM TEMP (DEG RANKIN)                          *
C*       MUIN - FREE STREAM VISCOSITY (LB-SEC/SQ FT)                   *
C*        PIN - FREE STREAM PRESSURE (LB/SQ FT)                        *
C*        UIN - FREE STREAM VELOCITY (FT/SEC)                          *
C*        CSH - COEFF OF SPECIFIC HEAT W/ CONST PRESSURE (BTU/LB-R)    *
C*         TR - WALL COOLING RATIO                                     *
C*          C - CHORD OF AIRFOIL (FT)                                  *
C*         RA - LEADING EDGE RADIUS (FT)                               *
C*          B - SPAN OF AIRFOIL (FT)                                   *
C*        REC - CRITICAL REYNOLDS NO.                                  *
C*        CPU - PRESSURE COEFF UPPER SURFACE                           *
C*        CPL - PRESSURE COEFF LOWER SURFACE                           *
C*         XU - UPPER SURFACE COORDINATE (FT)                          *
C*         XL - LOWER SURFACE COORDINATE (FT)                          *
C*        UEU - UPPER SURFACE VELOCITY (FT/SEC)                        *
C*        UEL - LOWER SURFACE VELOCITY (FT/SEC)                        *
C*        STL - LAMINAR STANTON NO.                                    *
C*        STT - TURBULENT STANTON NO.                                  *
C*        TAW - ADIABATIC WALL TEMP (DEG RANKIN)                       *
C*          H - HEAT TRANSFER COEFF (BTU/S-SQF-R)                      *
C*          Q - HEAT FLUX (BTU/SQF-S)                                  *
C*****************************************************************
```

```
      DIMENSION RE(2),CPU(21),CPL(21),UEU(21),UEL(21),TEU(21),TEL(21),
     *PEU(21),PEL(21),TAWU(21),TEKU(21),ROEU(21),REEU(21),TAWUL(21),
     *TEKUL(21),ROEUL(21),REEUL(21),TAWL(21),TEKL(21),XU(21),ROEL(21),
     *REEL(21),XL(21),TAWLL(21),TEKLL(21),ROELL(21),REELL(21),EML(21),
     *EMT(21),STL(21),HL(21),QEL(21),STT(21),HT(21),QET(21),HTL(21),
     *EMLL(21),EMTL(21),STLL(21),HLL(21),QELL(21),STTL(21),QETL(21),
     *QEU(23),QEB(23),X(23)
      REAL MULU(21),MULUL(21),MULL(21),MULLL(21),MUIN
      DATA GO/32.174/,R/1716./,CJ/778.16/,CSH/.24/,PR/.7/,C/.75/,B/1.83/
     *,RA/.025/,TIN/559.67/
      DATA XL/0.,.048,.086,.124,.163,.201,.238,.276,.313,.351,.389,.427,
     *.465,.503,.542,.580,.618,.656,.693,.731,.770/
      DATA XU/0.,.048,.086,.124,.163,.200,.238,.275,.313,.350,.388,.425,
     *.463,.500,.538,.575,.613,.651,.689,.728,.767/
      DATA CPL/1.000,-.265,-.455,-.340,-.325,-.315,-.280,-.250,-.260,
     *-.255,-.255,-.225,-.120,.085,.215,.270,.305,.330,.350,.350,.010/
      DATA CPU/1.000,-.645,-.600,-.580,-.540,-.490,-.455,-.450,-.445,
     *-.450,-.465,-.470,-.470,-.450,-.440,-.455,-.480,-.460,-.330,
     *-.075,.010/
      X(1)=0.
```


PROGRAM CONHEAT 74/74 OPT=1 FTN 4.5+414 09/09/77

```
      DO 5 JJ=2,21
    5 X(JJ)=X(JJ-1)+.05
   10 READ*,UIN,MUIN,PIN
      IF (EOF(5LINPUT).NE.0.) STOP "EOF ENCOUNTERED"
      READ*,NTR
      DO 700 II=1,NTR
      READ*,TR,REC
```

```
      PRINT 20,UIN,MUIN,PIN,TR
   20 FORMAT(//,1X,"FREE STREAM CONDITIONS-",/,5X,"VEL=",F8.3,3X,"MU=",
     *E11.5,/,5X,"P=",F9.3,2X,"TEMP RATIO=",F5.3,//)
      TW=TIN*TR
      RF(1)=SQRT(PR)
      RF(2)=PR**.333
      ROI=PIN/(R*TIN)
      REI=ROI*UIN*C/MUIN
      DO 100 I=1,21
      UEU(I)=UIN*SQRT(1.-CPU(I))
      UEL(I)=UIN*SQRT(1.-CPL(I))
      TEU(I)=TIN+(UIN**2.-UEU(I)**2.)/(2.*CSH*GO*CJ)
      TEL(I)=TIN+(UIN**2.-UEL(I)**2.)/(2.*CSH*GO*CJ)
      PEU(I)=PIN+(CPU(I)*ROI*UIN**2.)/2.
      PEL(I)=PIN+(CPL(I)*ROI*UIN**2.)/2.
  100 CONTINUE
C
C  DETERMINE UPPER SURFACE PROPERTIES
C
      DO 300 J=1,2
      DO 200 I=1,21
      TAWU(I)=TEU(I)+RF(J)*UEU(I)**2./(2.*CSH*GO*CJ)
      TEKU(I)=(TW+TEU(I))/2.+.22*(TAWU(I)-TEU(I))
      MULU(I)=.00000375*(TEU(I)/527.67)**1.5*(726.39/(TEU(I)+198.72))
      ROEU(I)=PEU(I)/(R*TEKU(I))
      REEU(I)=ROEU(I)*UEU(I)*XU(I)/MULU(I)
      IF (J.NE.1) GO TO 200
      RECRITU=ROI*UIN*XU(I)/MUIN
      K=I
      IF (RECRITU.GE.REC.OR.K.EQ.21) GO TO 140
      GO TO 200
  140 DO 150 L=1,K
      TAWUL(L)=TAWU(L)
      TEKUL(L)=TEKU(L)
      MULUL(L)=MULU(L)
      ROEUL(L)=ROEU(L)
```

```
      REEUL(L)=REEU(L)
  150 CONTINUE
      GO TO 300
  200 CONTINUE
  300 CONTINUE
C
C  DETERMINE LOWER SURFACE PROPERTIES
C
      DO 500 J=1,2
      DO 400 I=1,21
      TAWL(I)=TEL(I)+RF(J)*UEL(I)**2./(2.*CSH*GO*CJ)
      TEKL(I)=(TW+TEL(I))/2.+.22*(TAWL(I)-TEL(I))
      MULL(I)=.0000003775*(TEL(I)/527.67)**1.5*(726.39/(TEL(I)+198.72))
      ROEL(I)=PEL(I)/(R*TEKL(I))
```



```
      REEL(I)=ROEL(I)*UEL(I)*XL(I)/MULL(I)
      IF (J.NE.1) GO TO 400
      RECRITL=ROI*UIN*XL(I)/MUIN
      M=I
      IF (RECRITL.GE.REC.OR.M.EQ.21) GO TO 340
      GO TO 400
  340 DO 350 L=1,M
      TAWLL(L)=TAWL(L)
      TEKLL(L)=TEKL(L)
      MULLL(L)=MULL(L)
      ROELL(L)=ROEL(L)
      REELL(L)=REEL(L)
  350 CONTINUE
```

```
      GO TO 500
  400 CONTINUE
  500 CONTINUE
C
C  COMPUTE UPPER HEAT TRANSFER
C
      FML(1)=0. $ QUL=0.
      FMT(1)=0. $ QUT=0.
      STL(1)=0. $ STT(1)=0.
      HL(1)=GO*CSH*SQRT((5.74*UIN*MULUL(1)*ROEUL(1))/RA)*0.418
      QFL(1)=HL(1)*(TW-TAWUL(1))
      DO 550 I=2,21
      IF (I.GE.K.AND.K.NE.21) GO TO 520
      FML(I)=FML(I-1)+(XU(I)-XU(I-1))*((ROEUL(I)*UEU(I))**1.87+(ROEUL(I-
     *1)*UEU(I-1))**1.87)/2.
      STL(I)=0.418*SQRT(MULUL(I))*(ROEUL(I)*UEU(I))**.435/SQRT(
     *FML(I))
      HL(I)=STL(I)*ROEUL(I)*UEU(I)*CSH*GO
      QFL(I)=HL(I)*(TW-TAWUL(I))
      QUL=QUL+((XU(I)-XU(I-1))*B/2.*(QFL(I)+QFL(I-1)))
  520 FMT(I)=FMT(I-1)+(XU(I)-XU(I-1))*(ROEU(I)*UEU(I)+ROEU(I-1)*UEU(I-1)
     *)/2.
      IF (I.LT.K.OR.K.EQ.21) GO TO 550
      STT(I)=.0296*MULU(I)**.2*(1./PR)**.4)/FMT(I)**.2
      HT(I)=STT(I)*ROEU(I)*UEU(I)*CSH*GO
      QFT(I)=HT(I)*(TW-TAWU(I))
      QUT=QUT+((XU(I)-XU(I-1))*B/2.*(QFT(I)+QFT(I-1)))
  550 CONTINUE
C
C  COMPUTE LOWER HEAT TRANSFER
C
      FMLL(1)=0. $ QLL=0.
      FMTL(1)=0. $ QLT=0.
      STLL(1)=0. $ STTL(1)=0.
      HLL(1)=GO*CSH*SQRT((5.74*UIN*MULLL(1)*ROELL(1))/RA)*0.418
      QFLL(1)=HLL(1)*(TW-TAWLL(1))
```

```
      DO 600 I=2,21
      IF (I.GE.M.AND.M.NE.21) GO TO 570
      FMLL(I)=FMLL(I-1)+(XL(I)-XL(I-1))*((ROELL(I)*UEL(I))**1.87+(ROELL
     *(I-1)*UEL(I-1))**1.87)/2.
      STLL(I)=0.418*SQRT(MULLL(I))*(ROELL(I)*UEL(I))**.435/SQRT(
     *FMLL(I))
      HLL(I)=STLL(I)*ROELL(I)*UEL(I)*CSH*GO
      QFLL(I)=HLL(I)*(TW-TAWLL(I))
```

PROGRAM CONHEAT 74/74 OPT=1 FTN 4.5+414 09/09/77

```
      QLL=QLL+((XL(I)-XL(I-1))*B/2.*(QFLL(I)+QFLL(I-1)))
  570 FMTL(I)=FMTL(I-1)+(XL(I)-XL(I-1))*(ROEL(I)*UEL(I)+ROEL(I-1)
     **UEL(I-1))/2.
      IF (I.LT.M.OR.M.EQ.21) GO TO 600
      STTL(I)=.0295*MULL(I)**.2*(1./PR**.4)/FMTL(I)**.2
      HTL(I)=STTL(I)*ROEL(I)*UEL(I)*CSH*GO
      QFTL(I)=HTL(I)*(TW-TAWL(I))
      QLT=QLT+((XL(I)-XL(I-1))*B/2.*(QFTL(I)+QFTL(I-1)))
  600 CONTINUE
      QTOT=QUL+QUT+QLL+QLT
      PRINT 620
  620 FORMAT(3X,"XU(FT)",7X,"VEL(F/S)",5X,"RE AT EDGE",6X,"ST.NO.",4X,
     *"H(BTU/S-SQF-R)",1X,"Q(BTU/SQF-S)")
      KK=K-1
      IF (K.EQ.21) KK=K
      DO 630 I=1,KK
      QFU(I)=QFL(I)
  630 PRINT 650,XU(I),UEU(I),REFUL(I),STL(I),HL(I),QFL(I)
      IF (K.EQ.21) GO TO 655
```

```
      DO 640 I=K,21
      QFU(I)=QFT(I)
  640 PRINT 650,XU(I),UEU(I),REEU(I),STT(I),HT(I),QFT(I)
  650 FORMAT(1X,6(E10.4,4X))
      PRINT 660
  660 FORMAT(3X,"XL(FT)",7X,"VEL(F/S)",5X,"RE AT EDGE",6X,"ST.NO.",4X,
     *"H(BTU/S-SQFT-R)",1X,"Q(BTU/SQFT-S)")
      MM=M-1
      IF (M.EQ.21) MM=M
      DO 670 I=1,MM
      QFB(I)=QFLL(I)
  670 PRINT 650,XL(I),UEL(I),REELL(I),STLL(I),HLL(I),QFLL(I)
      IF (M.EQ.21) GO TO 685
      DO 680 I=M,21
      QFB(I)=QFTL(I)
  680 PRINT 650,XL(I),UEL(I),REEL(I),STTL(I),HTL(I),QFTL(I)
  685 PRINT 690,QTOT
  690 FORMAT(/,1X,"TOTAL HEAT FLOW IN BTU/SEC IS ",E10.4)
      CALL PLOT(6.,-12.,-3)
      CALL PLOT(2.,1.5,-3)
      CALL RECT(0.,0.,5.,6.,0.,3)
      CALL PLOT(.7,7.4,-3)
      CALL SCALE(X,5.,21,1)
      CALL SPAXIS(0.,0.,20HX/C (LOCATION/CHORD),-20,5.,0.,X(22),X(23),
     *1.45,.1,.105,0.,.5,2,.07)
      CALL SCALE(QFB,7.,21,1)
      CALL SPAXIS(0.,-7.,31HAIRFOIL HEAT FLUX (BTU/SEC-SQF),31,7.,90.,
     *QFB(22),QFB(23),-.8,-5.13,.105,90.,.5,2,.07)
      QFU(22)=QFB(22)
      QFU(23)=QFB(23)
      CALL PLOT(0.,-7.,-3)
      CALL LINE(X,QFU,21,1,1,1)
      CALL LINE(X,QFB,21,1,1,2)
      CALL PLOT(0.,7.,-3)
      CALL SYMBOL(1.76,-5.95,.105,1.0,,-1)
      CALL SYMBOL(1.98,-6.,.105,13HUPPER SURFACE,0.,13)
```

```
      CALL SYMBOL(1.76,-6.15,.105,2,0.,-1)
      CALL SYMBOL(1.98,-6.2,.105,13HLOWER SURFACE,0.,13)
```

PROGRAM CONHEAT 74/74 OPT=1 FTN 4.5+414 09/09/77

```
      CALL PLOTE(N)
  700 CONTINUE
      GO TO 10
      END
```

Appendix B

Convection Program Output

The computer program, CONHEAT, which was discussed in Section II and Appendix A was run with the proposed test data discussed in Section V. These results predict the heat transfer and flow properties for the proposed test conditions at a Mach number of 0.7. An example of the tabular results is contained in Table III. Plots of heat flux for all of the proposed cooling ratios are contained in Fig 13 through Fig 19.

Table III

Airfoil Local Properties at the Test Condition

$M=0.7$, $Re=1.673 \times 10^6$, $T_w/T_\infty = 0.824$

FREE STREAM CONDITIONS-
VEL= 813.69 MU= .37049E-06
P= 1323.488 TEMP RATIO= .824

XU(FT)	VEL(F/S)	RE AT EDGE	ST.NO.	H(BTU/S-SQF-R)	Q(BTU/SQF-S)
0.	0.	0.	0.	.3968E-01	-.6091E+01
.4330E-01	.1043E+04	.1577E+06	.1403E-02	.1409E-01	-.1955E+01
.8610E-01	.1023E+04	.2827E+06	.9284E-03	.9326E-02	-.1228E+01
.1240E+00	.1022E+04	.4077E+06	.7312E-03	.5952E-02	-.9699E+00
.1670E+00	.1009E+04	.5357E+06	.6212E-03	.5932E-02	-.8265E+00
.2010E+00	.9923E+03	.6565E+06	.5531E-03	.5296E-02	-.7421E+00
.2380E+00	.9807E+03	.7801E+06	.5020E-03	.4817E-02	-.6760E+00
.2750E+00	.9790E+03	.9011E+06	.4633E-03	.4442E-02	-.6241E+00
.3130E+00	.9774E+03	.1022E+07	.4316E-03	.4139E-02	-.5816E+00
.3510E+00	.9790E+03	.1147E+07	.4060E-03	.3893E-02	-.5469E+00
.3880E+00	.9861E+03	.1272E+07	.3838E-03	.3678E-02	-.5102E+00
.4250E+00	.9956E+03	.1394E+07	.3654E-03	.3502E-02	-.4913E+00
.4630E+00	.9953E+03	.1519E+07	.3493E-03	.3348E-02	-.4695E+00
.5010E+00	.9790E+03	.1638E+07	.3356E-03	.3218E-02	-.4521E+00
.5380E+00	.9757E+03	.1762E+07	.3231E-03	.3098E-02	-.4356E+00
.5750E+00	.9807E+03	.1881E+07	.3130E-03	.3027E-01	-.2541E+01
.6130E+00	.9891E+03	.2008E+07	.1883E-02	.1800E-01	-.2600E+01
.6510E+00	.9790E+03	.2129E+07	.1865E-02	.1781E-01	-.2575E+01
.6890E+00	.9777E+03	.2254E+07	.1849E-02	.1764E-01	-.2566E+01
.7260E+00	.8439E+03	.2366E+07	.1838E-02	.1716E-01	-.2521E+01
.7630E+00	.8090E+03	.2341E+07	.1812E-02	.1676E-01	-.2471E+01

XL(FT)	VEL(F/S)	RE AT EDGE	ST.NO.	H(BTU/S-SQF-R)	Q(BTU/SQF-S)
0.	0.	0.	0.	.3968E-01	-.6091E+01
.4330E-01	.9165E+03	.1567E+06	.1503E-02	.1432E-01	-.2045E+01
.8500E-01	.9817E+03	.2819E+06	.9283E-03	.8900E-02	-.1250E+01
.1241E+00	.9412E+03	.4031E+06	.7341E-03	.7044E-02	-.9965E+00
.1630E+00	.9295E+03	.5291E+06	.6227E-03	.5973E-02	-.8458E+00
.2010E+00	.9326E+03	.6517E+06	.5519E-03	.5293E-02	-.7500E+00
.2380E+00	.9193E+03	.7687E+06	.5024E-03	.4812E-02	-.6833E+00
.2760E+00	.9091E+03	.8880E+06	.4633E-03	.4471E-02	-.6304E+00
.3130E+00	.9126E+03	.1008E+07	.4327E-03	.4140E-02	-.5807E+00
.3510E+00	.9109E+03	.1130E+07	.4063E-03	.3892E-02	-.55 E+00
.3901E+00	.9104E+03	.1252E+07	.3851E-03	.3684E-02	-.5240E+00
.4270E+00	.8963E+03	.1369E+07	.3687E-03	.3500E-02	-.4993E+00
.4650E+00	.8805E+03	.1484E+07	.3537E-03	.3318E-02	-.4756E+00
.5030E+00	.7777E+03	.1583E+07	.3344E-03	.3047E-02	-.4427E+00
.5420E+00	.7204E+03	.1644E+07	.3193E-03	.2798E-02	-.4096E+00
.5810E+00	.6847E+03	.1711E+07	.1931E-02	.1657E-01	-.2470E+01
.6190E+00	.6773E+03	.1787E+07	.1909E-02	.1615E-01	-.2409E+01
.6580E+00	.6666E+03	.1867E+07	.1888E-02	.1578E-01	-.2356E+01
.6970E+00	.6555E+03	.1946E+07	.1870E-02	.1549E-01	-.2311E+01
.7350E+00	.6566E+03	.1947E+07	.1853E-02	.1533E-01	-.2292E+01
.7730E+00	.8093E+03	.2350E+07	.1824E-02	.1587E-01	-.2487E+01

TOTAL HEAT FLOW IN BTU/SEC IS -.4049E+01

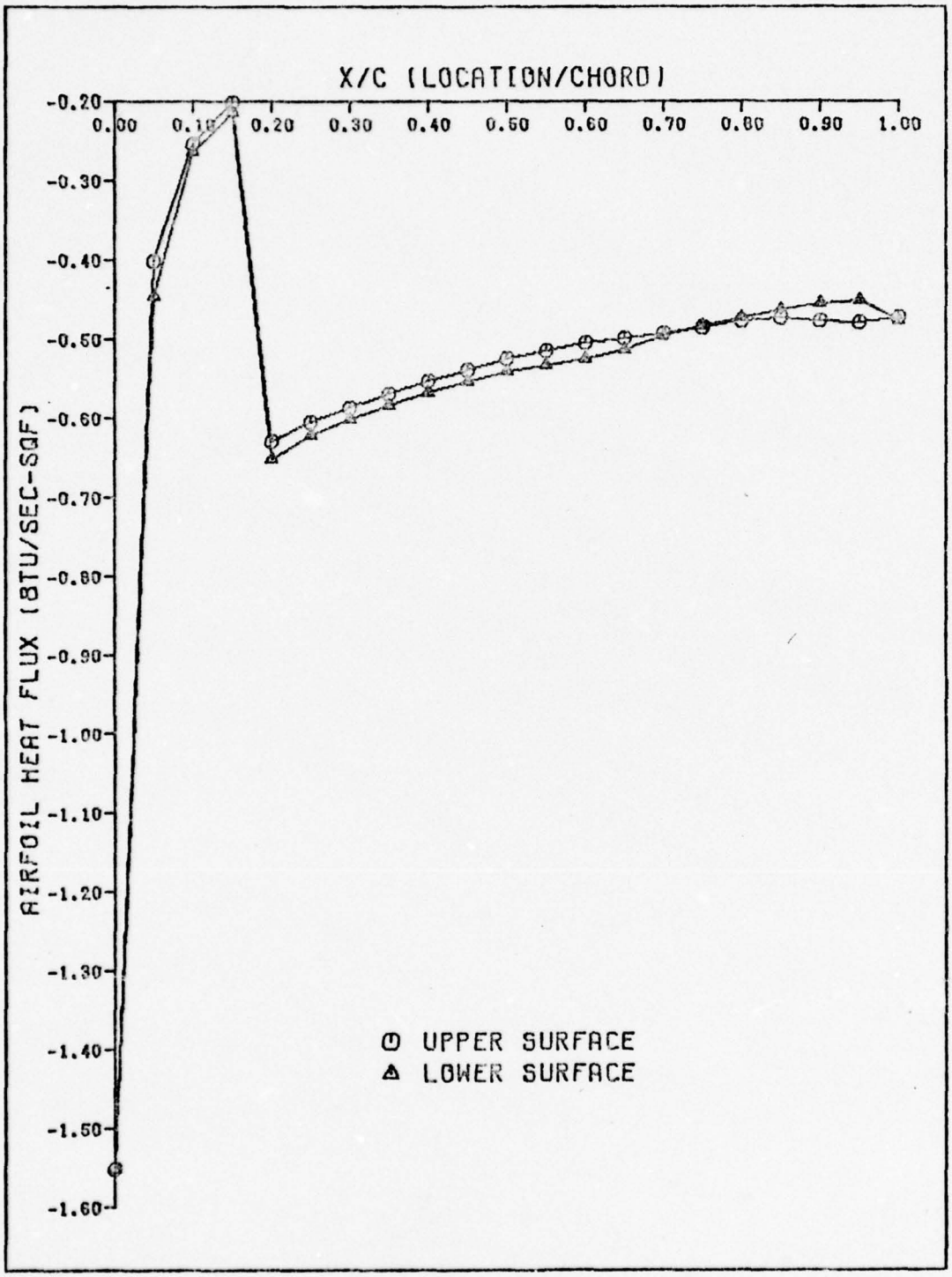

Fig.13 Airfoil Heat Flux at M=0.7, Re=0.923 x 10^6, and T_w/T_∞ =1.000

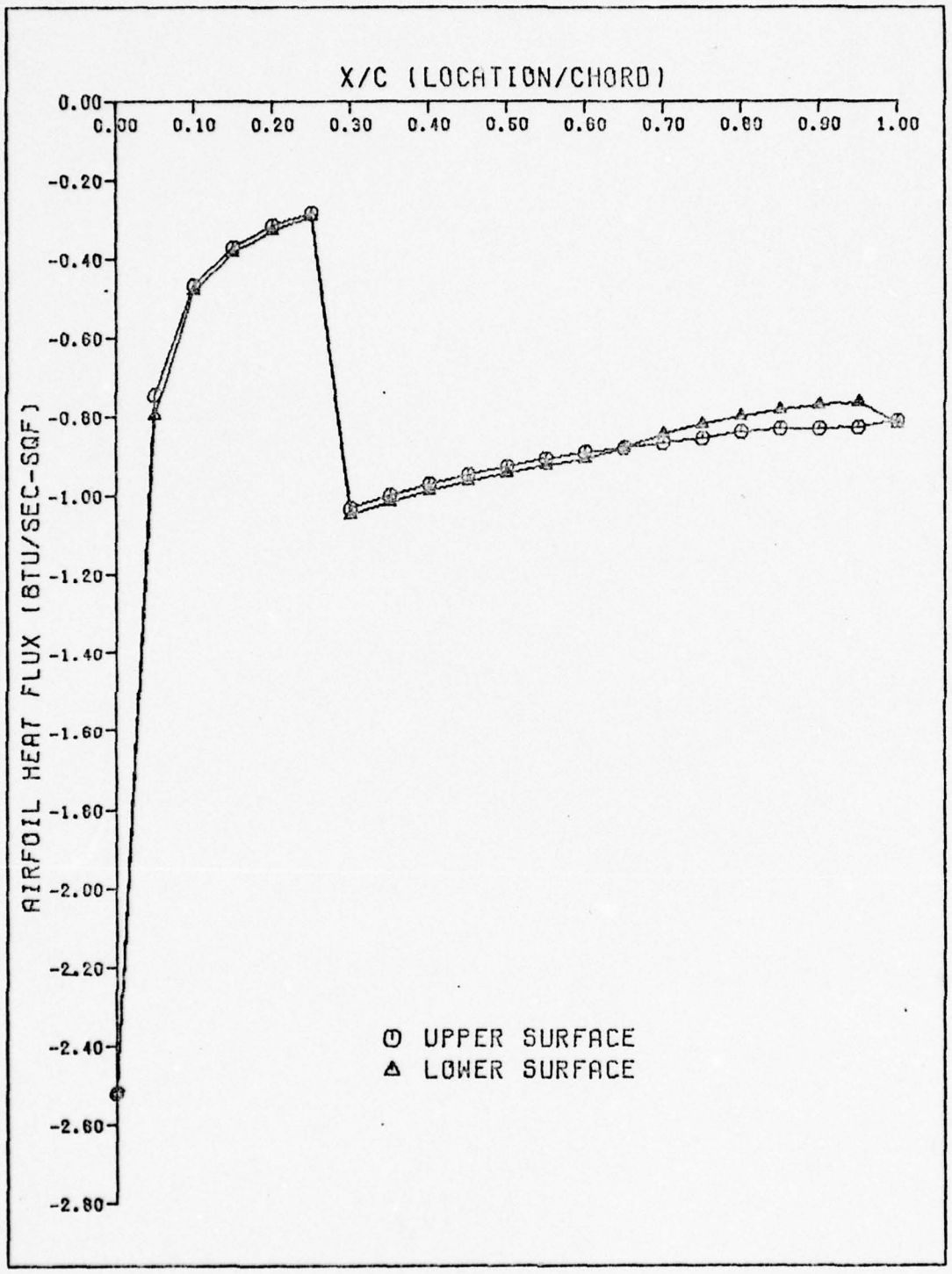

Fig.14 Airfoil Heat Flux at M=0.7, Re=0.923 x 10^6, and T_w/T_∞ =0.941

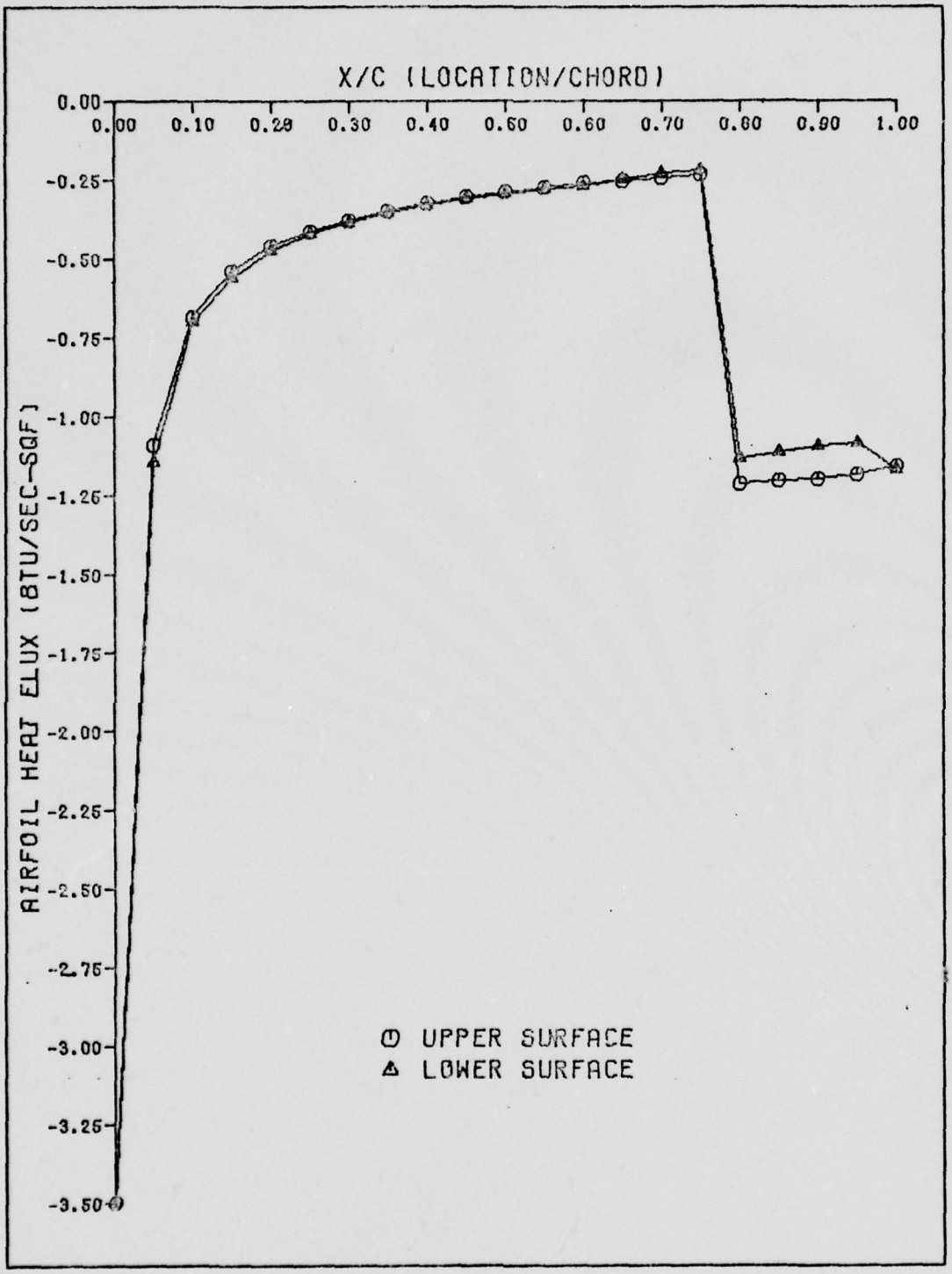

Fig.15 Airfoil Heat Flux at M=0.7, Re=0.923 x 10^6, and T_w/T_∞ =0.883

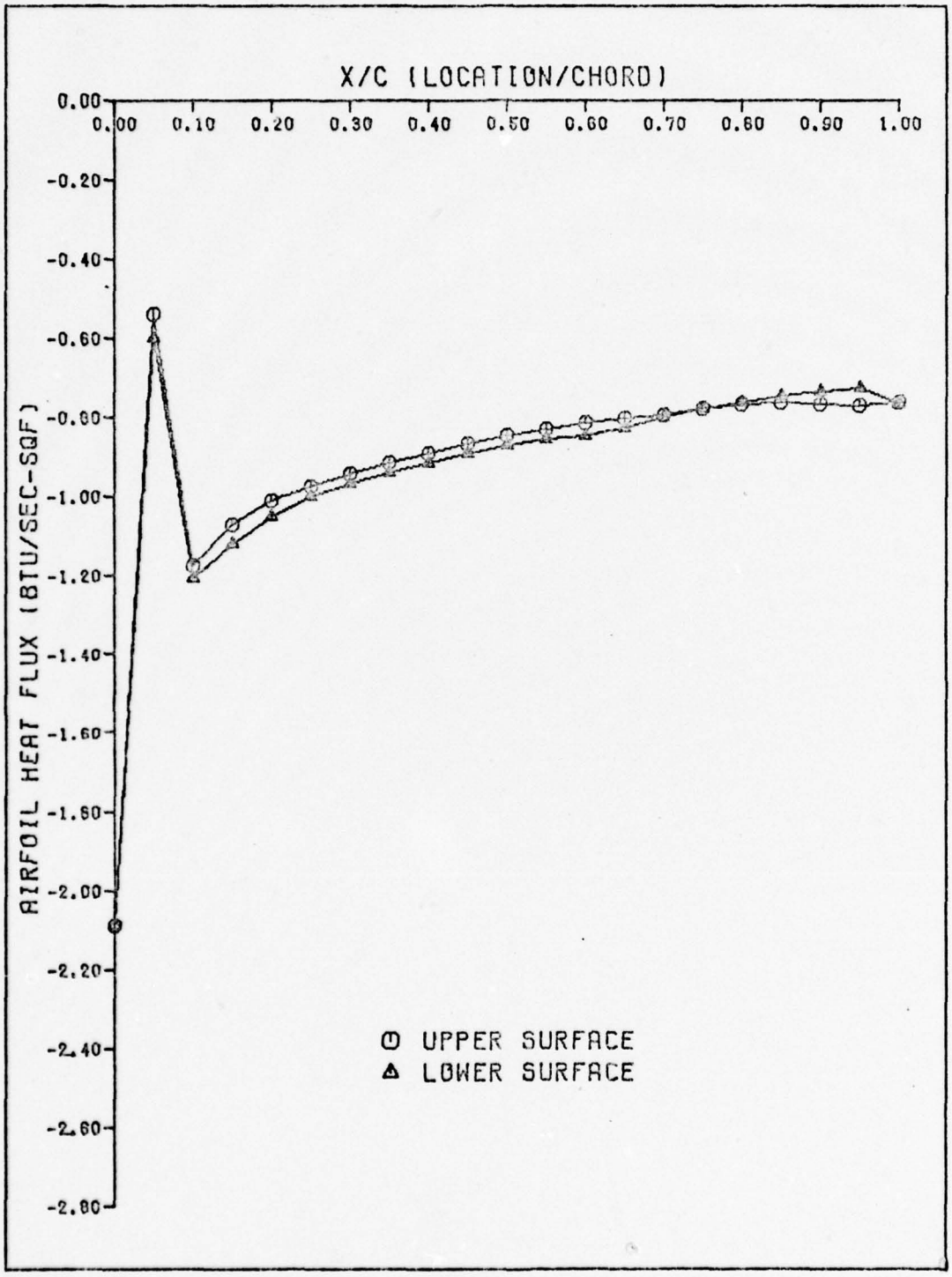

Fig. 16 Airfoil Heat Flux at M=0.7, Re=1.673 x 10^6, and T_w/T_∞ =1.000

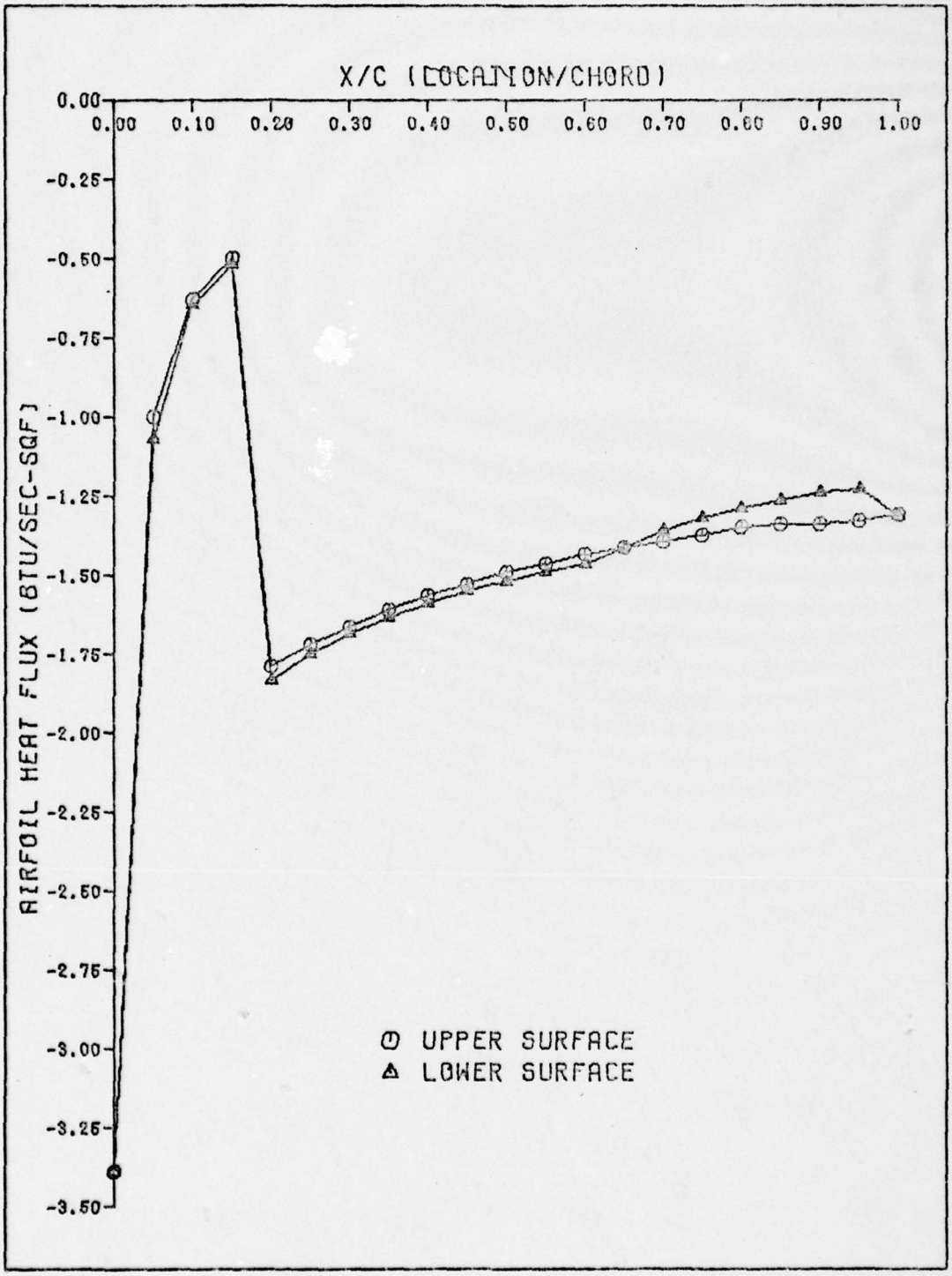

Fig. 17 Airfoil Heat Flux at M=0.7, Re=1.673 x 10^6, and T_w/T_∞ =0.941

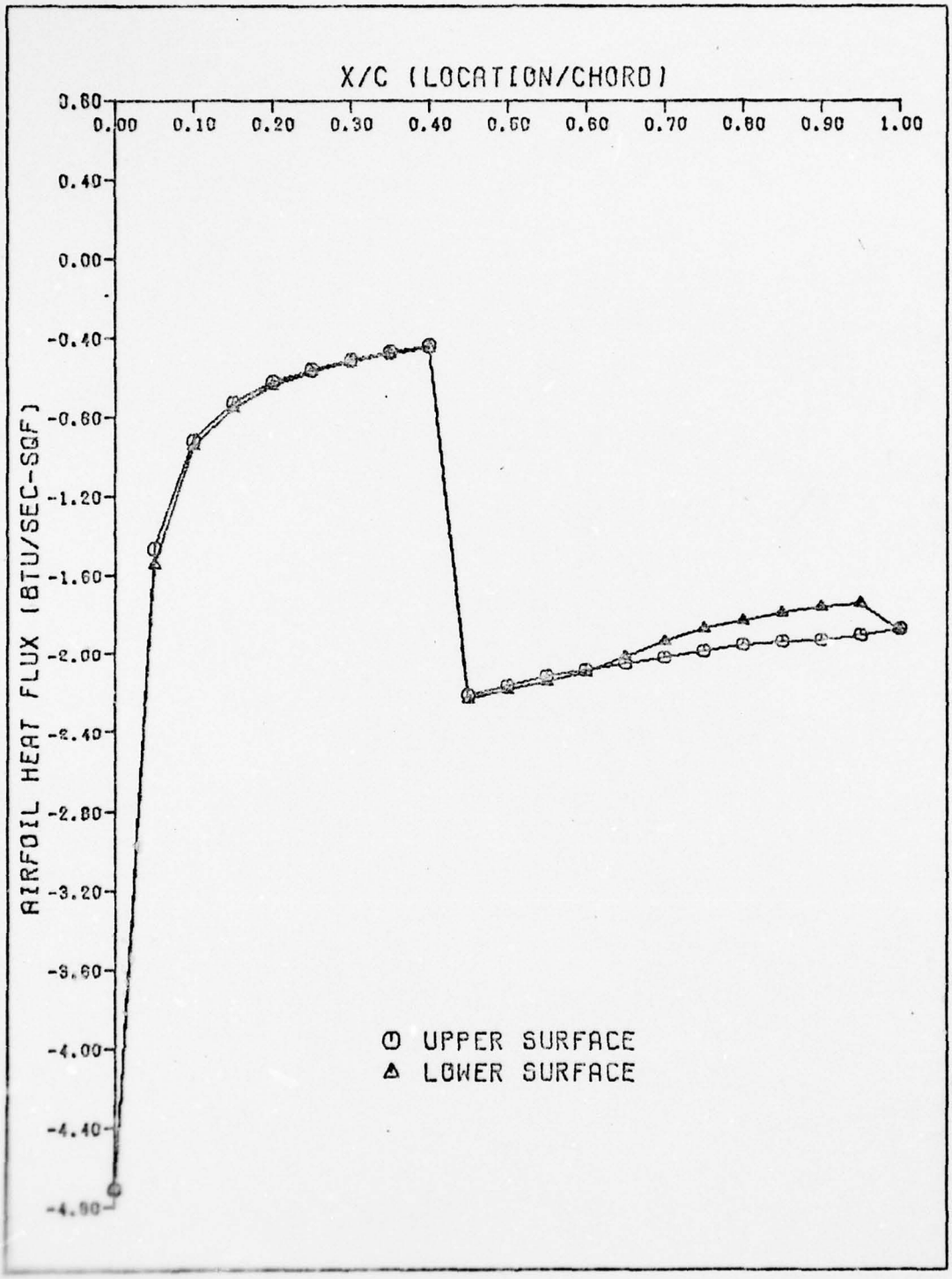

Fig. 18 Airfoil Heat Flux at M=0.7, Re=1.673 x 10^6, and T_w/T_∞ =0.883

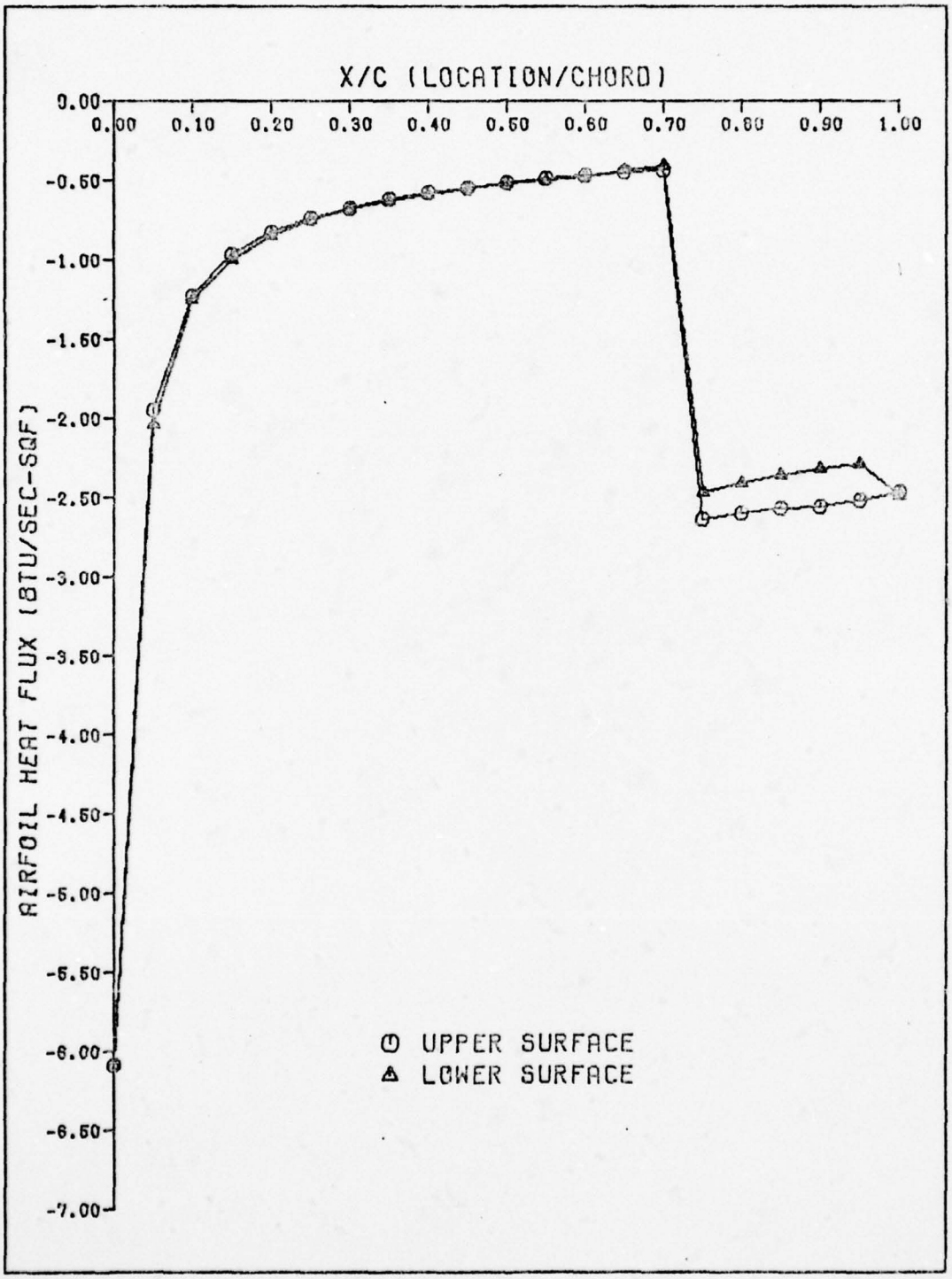

Fig. 19 Airfoil Heat Flux at M=0.7, Re=1.673 x 10^6, and T_w/T_∞ =0.824

Appendix C

Stress Analysis Calculations

Airfoil

Moments of Inertia and Centroids. With the aid of a full scale drawing of the airfoil section such as Fig 10, the area, centroid, and moments of inertia about the leading edge were computed using Eq 21-26. Then, the parallel axis theorem was applied to get the moments of inertia for axes through the centroid and for the x-axis parallel to the chord. The results were:

$$A = 3.430 \text{ in.}^2$$
$$C_x = 3.947 \text{ in.}$$
$$C_y = 0.042 \text{ in.}$$
$$I_x = 0.1187 \text{ in.}^4$$
$$I_y = 17.0948 \text{ in.}^4$$
$$I_{xy} = 0.3940 \text{ in.}^4$$

Material Selection. The materials used for the construction of the airfoil and end sections are listed in Table VII. A complete listing of structural properties needed to perform the entire stress analysis is included in Table IV by type of material.

Equivalent Force System. The computed uniform lift force at the design condition was 12.458 lb_f/in. of span for a total of 299 lb_f normal to the chord. The uniformly distributed drag force was 0.537 lb_f/in. of span for a total force

Table IV

Structural Limits of Materials

Type Material	Tension*		Compression*		Shear*	
	Yld	Ult	Yld	Ult	Yld	Ult
2024-T4 Alum (Ref 9:85)	40	64	38	@	23	40
AISI-SAE-4130 Steel (Ref 14:452)	117	136	@	136	@	102
Oak, White (Ref 9:146)	@	0.8	@	@	@	2

Yld - Yield
Ult - Ultimate

* All stresses in 1000 psi
@ Not available

of 12.9 lb_f. The moment of 672 in.-lb_f was distributed uniformly at 28.00 in.lb_f/in. of span. These are the theoretical loads computed in Section III. This system of forces was concurrent at the quarter chord point.

Critical Points. Due to model symmetry, only half of the airfoil had to be analyzed. There were 5 critical points selected:

1. Mid-span
2. 4.5 in. from mid-span
3. Center of airfoil boss
4. 11.0 in. from mid-span
5. End of span

Special Considerations. The elliptical shell which replaced the airfoil section for the analysis had a wall thickness of 0.229 in. for a 9 in. major axis and 0.99 in.

minor axis. The ellipse was defined by solving the following equation for thickness, t:

$$\text{Area of Ellipse} = \pi[ab-(a-t)(b-t)] = 3.43 \text{ in.}^2$$

Equation 27 was used to compute the shear stress at critical points 1 through 4. Equation 28 was used at point number 5 for the shear stress of the solid elliptical section.

Stresses and Safety Factors. The airfoil was assumed to behave as a simple beam with a uniform load and symmetrically overhanging ends. The normal and shear stresses were computed for 4 locations at each critical point: the leading edge, trailing edge, top of the section at maximum thickness, and bottom of the section at maximum thickness. The stresses were combined using Eq 30 and 31. The safety factors were computed with Eq 32. These results are in Table V.

Mounting Struts

Moments of Inertia and Centroids. The vertical portion of the strut was assumed to resist bending with the exhaust pipe only. The moment of inertia of the 3/4 in., nominal sized pipe was 0.0448 in.^{4} The moment of inertia and centroid of the horizontal portion was computed using Eq 21-26 with the drawing of the cross-section of the strut in Fig 7. The result was an area of 0.8402 in.^{2}, the centroid which was 0.500 in. from the center of the exhaust pipe, and the moment of inertia which was 0.272 in.^{4} about the axis perpendicular to the axis of symmetry of the section.

Material Selection. The materials used for the con-

Table V

Maximum Stresses and Safety Factors

for the Airfoil

Critical Point		σ_{max}	τ_{max}	FS	FS
#	LOCATION	10^2psi	10^2psi	YIELD	ULTIMATE
	Top	32.973	24.418	7.4	12.5
1	Bottom	14.873	25.101	8.7	@
	Front	0.461	0.483	415.2	@
	Back	0.512	0.483	408.3	707.1
	Top	19.140	12.991	13.5	22.7
2	Bottom	6.279	13.571	16.3	@
	Front	0.389	0.405	500.0	@
	Back	0.426	0.405	488.0	845.2
	Top	0.086	1.155	200.0	@
3	Bottom	2.609	1.431	114.4	189.7
	Front	0.439	0.436	461.3	816.5
	Back	0.432	0.436	466.3	@
	Top	4.967	5.086	39.4	@
4	Bottom	5.228	5.087	38.1	66.2
	Front	0.144	0.144	1581.3	2786.3
	Back	0.143	0.144	1581.3	@
5	Top	0.	0.485	@	41.2

@ Not computed

struction of the strut are listed in Table VII. The structural limits of these materials are in Table IV. The epoxy casing material was not used to support loads in the analysis.

Equivalent Force System. Due to the model symmetry, only half of the loads used to analyze the airfoil acted on each vertical portion of the strut. The strut drag of 7.27 lb_f which acted at the middle of the strut was added to the system. To obtain a concurrent force system, the strut drag was moved parallel to the location of the airfoil chordline, and a couple equal to the drag force times the translated distance was also added. The resulting equivalent system was the following:

$$L = 149.5\ lb_f$$

$$D = 13.7\ lb_f$$

$$M = 291.5\ in.\text{-}lb_f$$

This equivalent system for the vertical portion was translated in a similar manner to obtain the forces and moment acting on the horizontal portion. Upon translation to the base of the vertical portion, the resulting equivalent system for the horizontal portion was:

$$L = 149.5\ lb_f$$

$$D = 13.7\ lb_f$$

$$M = 442.4\ in.\text{-}lb_f$$

Critical Points. There were only two critical points to analyze on the strut. These were the points of maximum bending moment. One point was 11.0 in. down from the airfoil chordline on the vertical portion of the strut. The other

point was 23.973 in. from the center of the vertical exhaust pipe.

Special Considerations. The computed normal stress on the vertical portion of the strut was corrected for curvature affects. The normal stress was multiplied by a correction factor on the inside and outside of the curve which were 1.70 and 0.71, respectively.

Stresses and Safety Factors. Both portions of the strut were assumed to be cantilever beams with concentrated loads at the free end. The stresses were computed for 2 locations, front and rear, at each critical point. The stresses were combined by Eq 30 and 31, and safety factors were computed with Eq 32. On the inside of the vertical strut, the maximum normal stress was -8549 psi, the maximum shear stress was 4275 psi, and the ultimate safety factor was 13.2. On the outside of the vertical strut, the maximum normal stress was 3916 psi, the maximum shear stress was 1958 psi, and the ultimate safety factor was 28.89. On the top of the horizontal strut, the maximum normal stress was -18,076 psi, the maximum shear stress was 9030 psi, and the ultimate safety factor was 6.3. On the bottom of the horizontal strut, the maximum normal stress was 15,158 psi, the maximum shear stress was 1580 psi, and the safety factor was 7.47.

Mounting Boss

Moments of Inertia and Centroids. Due to the nature of the assumed equivalent force system, no moments of inertia

or centroids were calculated.

Material Selection. The material used to construct the mounting boss was 2024-T4 aluminum. This material's structural limits are listed in Table IV. The 6-40 machine screws used had an ultimate stress limit of 54,400 psi. The ultimate shear stress for the fillet weld was 11,300 psi.

Equivalent Force System. The same loads that acted on the vertical portion of the strut also acted on the mounting boss. However, the drag was neglected since it was much smaller than the lift force. The moment was replaced by an equivalent force and moment arm. The result which was the sum of the lift and equivalent force was 455.7 lb_f.

Critical Points. There were three critical points on the mounting boss. These points were the screws which fastened the boss to the airfoil and boss plate, the flange of the boss, and the boss plate fillet weld.

Stresses and Safety Factors. There were 11 screws fastening the boss to the airfoil and 11 screws fastening the boss to the boss plate. The maximum stress on the screws was 4102 psi, and the ultimate safety factor was 13.3. The maximum shear stress on the flange of the boss which was corrected for stress concentration was 890 psi. The yield safety factor was 44.9. The maximum shear stress on the fillet weld was 1032 psi, and the ultimate safety factor was 43.8. These stresses and safety factors were computed with Eq 29 through Eq 32.

Mounting Plate

Moments of Inertia and Centroids. Due to the nature of the equivalent force system, no moments of inertia or centroids were calculated.

Material Selection. The material used to construct the mounting plate was 4130 low alloy steel. This material's structural limits are listed in Table IV. The fillet weld had an ultimate shear limit of 45,200 psi. The mounting bolts, 1/4 in. hexhead, had an ultimate normal stress of 44,800 psi and an ultimate shear stress of 33,600 psi.

Equivalent Force System. The equivalent force system was the same as the loads that acted on the horizontal portion of the strut.

Critical Points. There were two critical points. These points were the 1/8 in. fillet weld between the plate and the strut and the mounting bolts.

Stresses and Safety Factors. The stresses and safety factors were computed with Eq 29 through Eq 32. The maximum shear stress on the fillet weld was 7580 psi, and the ultimate safety factor was 6.0. The maximum normal stress on the mounting bolts was 1032 psi, and the maximum shear stress was 7580 psi. The ultimate safety factor on the bolts was 4.4.

Appendix D

Details of Model Construction

As a culmination of the design and analysis process, details necessary for the construction of the model have been specified. Figure 5, 7, 8, 9, 10, 20, and 21 depict all of the major parts that comprise the airfoil and strut mount system. Only Fig 20 and 21 appear in this appendix. Figure 20 contains a perspective of the entire assembly. Notes which explain special considerations during construction or clarify details have been included in the drawings. The airfoil section shape used is the McDonnell Douglas Corporation, DSMA 523, supercritical airfoil. Table VI provides geometric coordinates (Ref 8:738) necessary to contour the surface of the airfoil for a 9 inch chord.

Several items require special attention during construction. Teflon gaskets must be used on all contact surfaces between parts to prevent leakage of liquid and gaseous nitrogen. After the thermocouples have been installed using the 10-32 screws with the centers drilled as seen in Detail A of Fig 10, the centers must be back filled with epoxy to secure the thermocouple wires and insulate the thermocouple from direct contact with the liquid nitrogen.

Lastly, aluminumized milar and fiber glass multilayered insulation must be used to wrap all thermocouple wires and the liquid nitrogen supply line that leads to the mounting strut.

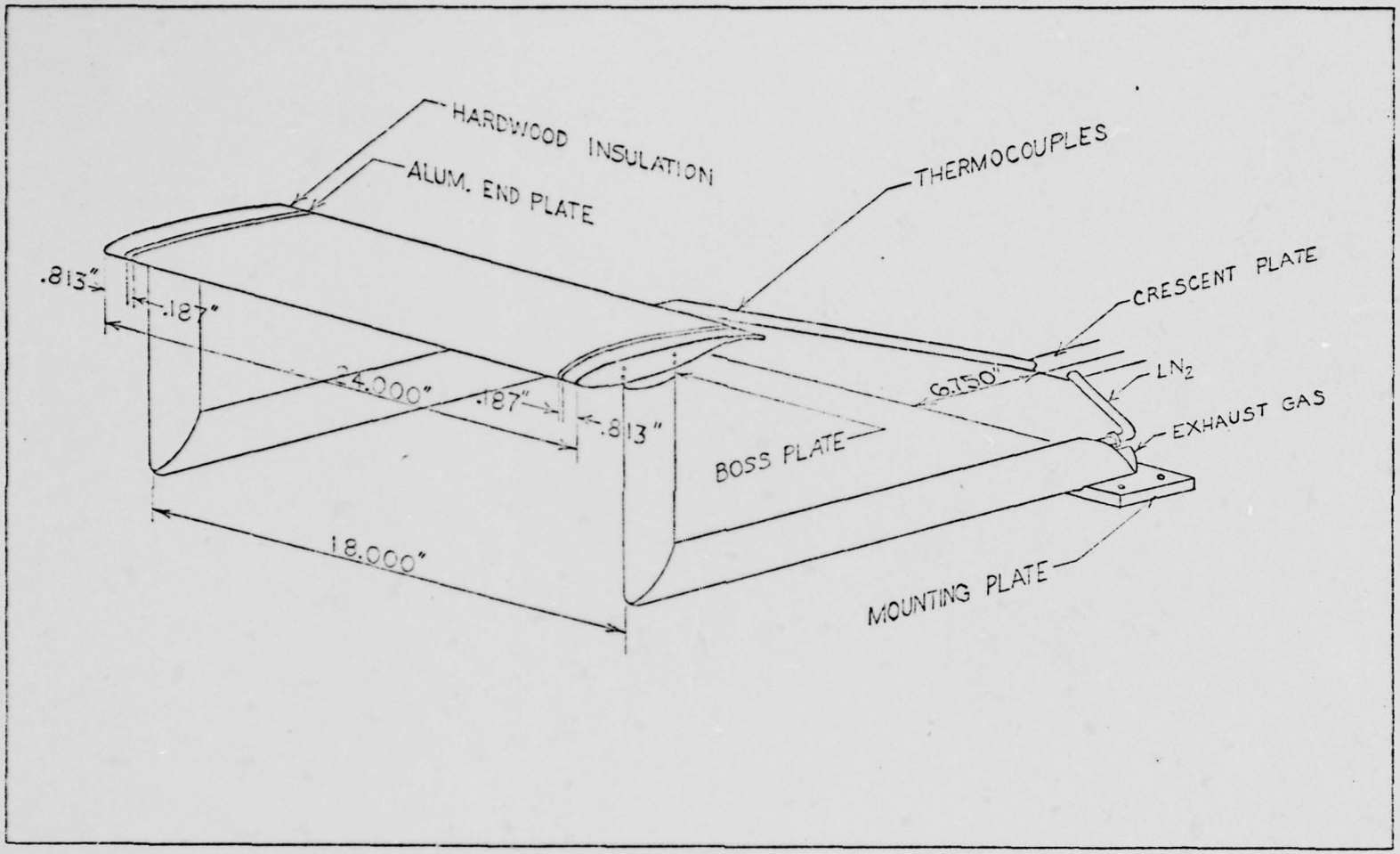

Fig. 20 Perspective View of Airfoil Model with Struts

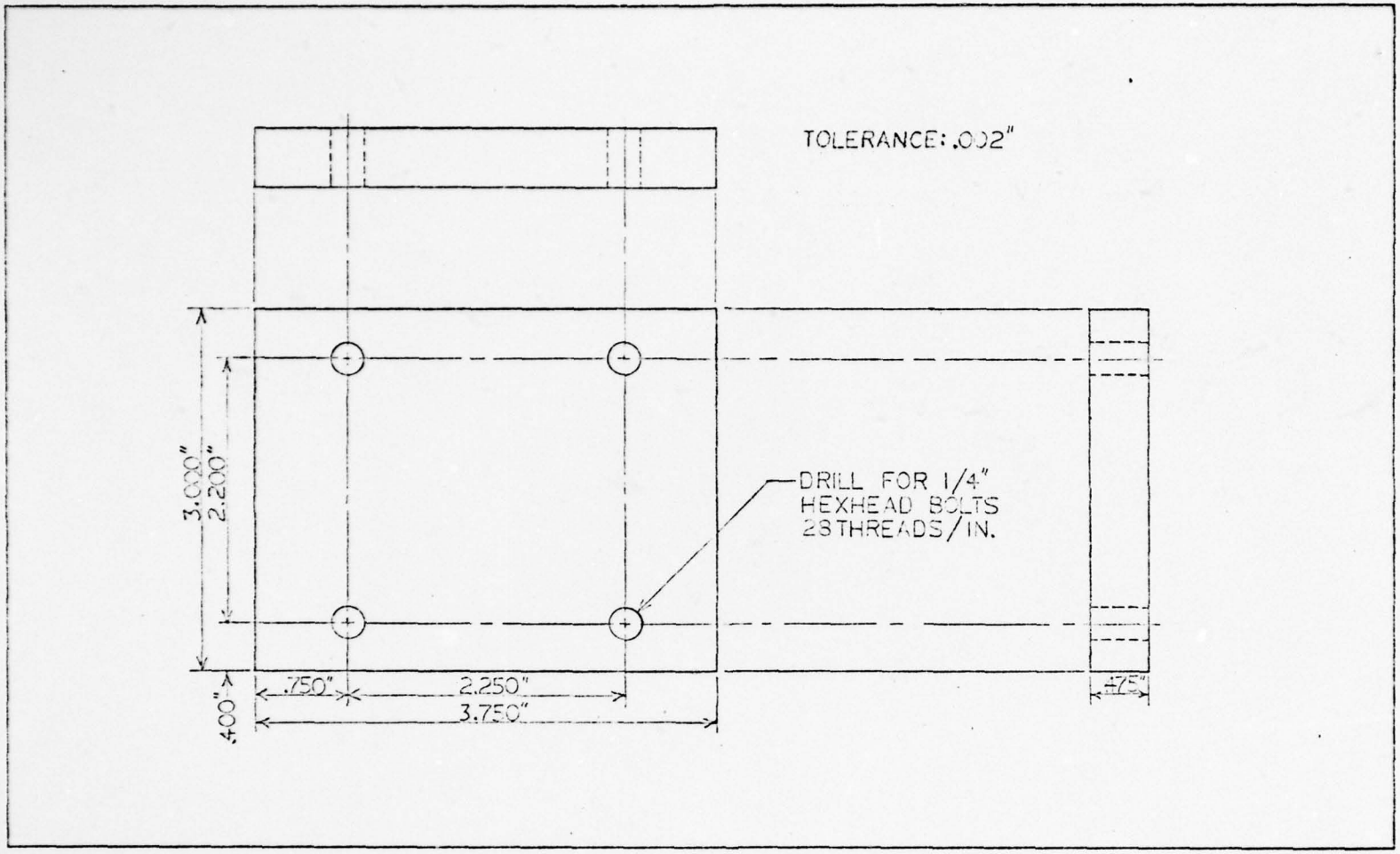

Fig. 21 Strut Mounting Plate

Table VI

Airfoil Section Coordinates

X	Y_U	Y_L	t	X	Y_U	Y_L	t
.0045	.0456	-.0459	.0915	4.1400	.4963	-.4693	.9656
.0090	.0639	-.0642	.1281	4.3200	.4948	-.4602	.9550
.0225	.0996	-.0997	.1993	4.5000	.4925	-.4492	.9417
.0450	.1379	-.1379	.2758	4.6800	.4895	-.4363	.9258
.0675	.1658	-.1658	.3316	4.8600	.4858	-.4210	.9068
.0900	.1864	-.1860	.3724	5.0400	.4814	-.4015	.8829
.1125	.2039	-.2029	.4068	5.2200	.4763	-.3781	.8544
.1350	.2184	-.2172	.4356	5.4000	.4704	-.3500	.8204
.1800	.2423	-.2407	.4830	5.5800	.4639	-.3166	.7805
.2700	.2766	-.2760	.5526	5.7600	.4565	-.2785	.7350
.3600	.3011	-.3025	.6036	5.9400	.4484	-.2375	.6859
.5400	.3367	-.3428	.6795	6.1200	.4395	-.1939	.6334
.7200	.3633	-.3757	.7390	6.3000	.4295	-.1526	.5821
.9000	.3869	-.4009	.7878	6.4800	.4184	-.1142	.5326
1.0800	.4068	-.4212	.8280	6.6600	.4062	-.0788	.4850
1.2600	.4232	-.4375	.8607	6.8400	.3926	-.0468	.4394
1.4400	.4369	-.4510	.8879	7.0200	.3775	-.0184	.3959
1.6200	.4485	-.4621	.9106	7.2000	.3604	.0062	.3542
1.8000	.4581	-.4713	.9294	7.3800	.3412	.0267	.3145
1.9800	.4662	-.4789	.9451	7.5600	.3195	.0428	.2767
2.1600	.4731	-.4850	.9581	7.7400	.2950	.0542	.2408
2.3400	.4788	-.4898	.9686	7.9200	.2670	.0602	.2068
2.5200	.4836	-.4933	.9769	8.1000	.2354	.0595	.1759
2.7000	.4874	-.4955	.9829	8.2800	.1997	.0507	.1490
2.8800	.4906	-.4965	.9871	8.4600	.1594	.0321	.1273
3.0600	.4931	-.4962	.9893	8.6400	.1138	.0031	.1107
3.2400	.4950	-.4948	.9898	8.8200	.0616	-.0379	.0995
3.4200	.4963	-.4923	.9886	9.0000	.0028	-.0910	.0938
3.6000	.4972	-.4885	.9857				
3.7800	.4974	-.4835	.9809				

All measurements in inches (accurate to 0.0001 in.)

AD-A048 895 AIR FORCE INST OF TECH WRIGHT-PATTERSON AFB OHIO SCH--ETC F/G 20/4
ANALYSIS AND DESIGN OF A COOLED SUPERCRITICAL AIRFOIL TEST MODE--ETC(U)
DEC 77 R G POPE

UNCLASSIFIED AFIT/GAE/AA/77D-11 NL

2 of 2
ADA048 895

END
DATE FILMED
2-78
DDC

Materials to be used for construction of the model were determined from consideration of the heat transfer and stress analysis. The thermal and structural properties of these materials were required to exceed the limits of the design condition. Table VII lists materials to be used for the components of the model.

Table VII

Specification of Construction Materials

Component	Material
Airfoil	
Center Section	2024-T4 Aluminum
End Plates	2024-T4 Aluminum
Insulating End Sections	White Oak (Hardwood)
Airfoil Bosses	2024-T4 Aluminum
Cooling Nozzles	Type 304 Stainless Steel
Strut Boss Plates	AISI-SAE4130 Low Alloy Steel
Mounting Struts	
Exhaust Pipes	AISI-SAE4130 Low Alloy Steel
Thermocouple and LN_2 Pipe	AISI-SAE4130 Low Alloy Steel
Reinforcing Bars	AISI-SAE4130 Low Alloy Steel
Contour Shape	C301 Epoxy (Aluminum Filled)
Strut Mounting Plates	AISI-SAE Low Alloy Steel
Thermocouple and LN_2 Supply Pipe	Type 304 Stainless Steel

The requirements for fastening methods were based on

the stress analysis. Two primary methods which will be employed are fillister head, fine thread, machine screws and fillet welds. Table VIII lists the fastening method with sizes for all of the components of the model.

Table VIII

Specification of Fasteners

Component Combination	Type Fastener	Size
Airfoil Center Section Halves	Fillister Screw	10-32
Airfoil End Plates and Insulating End Sections to Center Section	Fillister Screw	10-32
Airfoil Boss to Airfoil Center Section	Fillister Screw	6-40
Cooling Nozzles to Airfoil Boss	Fillister Screw	6-40
Airfoil Boss to Strut Boss Plate	Fillister Screw	6-40
Strut Boss Plate to Strut Pipe	Fillet Weld	1/8 in.
Reinforcing Bars to Exhaust Pipe	Fillet Weld	3/16 in.
Reinforcing Bars to LN_2 Pipe	Fillet Weld	3/32 in.
Struts to Mounting Plate	Fillet Weld	1/8 in.
Mounting Plate to Wind Tunnel	Hexhead Screw	1/4 in. 28 Threads per inch

VITA

Ray Glenn Pope, Jr. was born in Salisbury, North Carolina on 7 February 1949. He graduated from high school in Spencer, North Carolina in 1967 and from North Carolina State University from which he received the Bachelor of Science Degree in Aerospace Engineering in May 1971. He received a commission in the USAF through the ROTC program upon graduation and entered active duty in June 1971. After completing the Missile Maintenance Officers course at Chanute AFB, Illinois in September 1971, he served as a Combat Targeting Team Chief, Combat Targeting Team Instructor, and Combat Targeting Quality Control Inspector and Evaluator at F.E. Warren AFB, Wyoming. In June 1974 he was transferred to Malmstrom AFB, Montana where he served as the Assistant Chief of the Quality Control Division until entering the School of Engineering, Air Force Institute of Technology, in June 1976.

Permanent address: Route 3, Box 275B
Perry, Florida 32347

UNCLASSIFIED

SECURITY CLASSIFICATION OF THIS PAGE (When Data Entered)

(14) REPORT DOCUMENTATION PAGE

READ INSTRUCTIONS BEFORE COMPLETING FORM

1. REPORT NUMBER: AFIT/GAE/AA/77D-11

2. GOVT ACCESSION NO.

3. RECIPIENT'S CATALOG NUMBER

(9) Master's thesis,

4. TITLE (and Subtitle)

(6) ANALYSIS AND DESIGN OF A COOLED SUPERCRITICAL AIRFOIL TEST MODEL.

5. TYPE OF REPORT & PERIOD COVERED: MS Thesis

6. PERFORMING ORG. REPORT NUMBER

7. AUTHOR(s)

(10) Ray Glenn Pope, Jr
Capt.

8. CONTRACT OR GRANT NUMBER(s)

9. PERFORMING ORGANIZATION NAME AND ADDRESS

Air Force Institute of Technology (AFIT-EN)
Wright-Patterson AFB, Ohio 45433

10. PROGRAM ELEMENT, PROJECT, TASK AREA & WORK UNIT NUMBERS

11. CONTROLLING OFFICE NAME AND ADDRESS

Aeromechanics Division (FXE)
Air Force Flight Dynamics Laboratory
Wright-Patterson AFB, Ohio 45433

(11) 12. REPORT DATE: Dec [redacted] 77

13. NUMBER OF PAGES: ~~98~~ (12) 101p.

14. MONITORING AGENCY NAME & ADDRESS (if different from Controlling Office)

15. SECURITY CLASS. (of this report): Unclassified

15a. DECLASSIFICATION/DOWNGRADING SCHEDULE

16. DISTRIBUTION STATEMENT (of this Report)

Approved for public release; distribution unlimited.

17. DISTRIBUTION STATEMENT (of the abstract entered in Block 20, if different from Report)

18. SUPPLEMENTARY NOTES

Approved for public release: IAW AFR 190-17

JERRAL F. GUESS, Captain, USAF
Director of Information

19. KEY WORDS (Continue on reverse side if necessary and identify by block number)

Boundary Layer
Boundary Layer Transition
Convection (Heat Transfer)
Airfoils
Supercritical Airfoils

20. ABSTRACT (Continue on reverse side if necessary and identify by block number)

A wind tunnel test model of a supercritical airfoil was designed to investigate the wall cooling effect on subsonic boundary layer stability. A DSMA 523 airfoil section was employed. The model was designed to have surface temperature instrumentation and a liquid nitrogen cooling system.

Heat transfer, aerodynamic loads and stresses, and instrumentation were analyzed for the proposed test conditions. A computer program was developed to analyze the forced, →

DD FORM 1 JAN 73 1473 EDITION OF 1 NOV 65 IS OBSOLETE

UNCLASSIFIED

SECURITY CLASSIFICATION OF THIS PAGE (When Data Entered)

012 225

10 to the 6th power

convective heat transfer over a two-dimensional body with a constant wall temperature. The program utilized an integral method to compute local Stanton numbers. Local heat flux and total heat flow were predicted for a Mach number of 0.7, Reynolds numbers of 0.923 x 10^6 and 1.673 x 10^6, and cooling ratios from 1.000 to 0.824. The stress analysis consisted of applying beam bending theory, along with some simplifying assumptions, to the model. Construction drawings and specified test conditions for Mach numbers of 0.3, 0.5, and 0.7 are included. The proposed test are to be conducted in the subsonic test section of the Trisonic Test Facility at Wright-Patterson AFB, Ohio.